01188.67-002

Airborne Separation Assurance with Local TFM Conformance for Free Maneuvering Operations
FINAL REPORT

K. Tysen Mueller
David R. Schleicher

Seagull Technology, Inc.

Prepared for:
National Aeronautics and Space Administration
Ames Research Center, Moffett Field, CA

Under Subcontract to:
Systems Research Corporation Contract: NAS2-98005,
Seagull Subcontract: 99-0249, Task Order 1266-330

July 2002

Table of Contents

Table of Contents -- continued

Acknowledgements

The research described in this report was performed as Research Task Order 67 (RTO-67), under NASA contract: NAS2-98005. The authors wish to gratefully acknowledge the extensive direction and feedback provided by Dr. Karl Bilimoria, NASA Ames Research Center.

Tysen Mueller developed the conflict resolution algorithms, developed the Matlab test case simulations, and was the principal contributor to this report. David Schleicher analyzed the MD-80 maneuver envelope, real-world operational constraints, and provided editorial support and feedback.

1 Executive Summary

1.1 Background

The aircraft conflict detection and resolution (CD&R) literature has focused primarily on the conflict detection and avoidance problem. Less material has been presented on the recovery maneuvers required to complete the conflict resolution. Also, only limited research has been published that addresses the two-body CD&R problem in the presence of traffic flow constraints.

A number of different air traffic flow constraints are investigated. These traffic flow constraints include conflict avoidance of an intruder aircraft with recovery to a miles-in-trail (MIT) slot. In addition the recovery maneuver following conflict avoidance with an intruder aircraft or hazard region to meet a required time of arrival (RTA) at a stationary (next) waypoint is studied.

This report summarizes the conflict detection, avoidance, and recovery algorithms for two aircraft or an aircraft with a hazard region. Since the speed maneuver capability of an aircraft is limited, the available speed maneuver capability of a typical jet aircraft (MD-80) as a function of pressure altitude is computed.

To provide a quantitative comparison between alternate conflict resolution maneuver options, a maneuver efficiency metric is developed. This metric is sensitive to changes in the flight time and the fuel consumed during conflict resolution maneuvers. Using this efficiency metric based on the performance characteristics of an MD-80 aircraft, a number of test cases are evaluated consisting of two-aircraft conflict resolution maneuvers as well as maneuvers of a single aircraft around a hazard region. The nominal unconstrained maneuver cases are then compared to the RTA or MIT-constrained cases. The test cases involve both a single crossing angle scenario as well as parametric crossing angle scenarios. Also scenarios involving differences in the initial speed of the intruder aircraft are developed that provide a speed advantage / disadvantage to the own aircraft.

The conflict resolution maneuvers summarized in this report focus on the horizontal (planar) conflict scenario using maneuvers that involve the aircraft speed, track angle, or both. The focus of this report is on avoidance and recovery maneuvers that can be described by analytic or semi-analytic solutions. The change in speed or track angle is initially assumed to be completed in a short time relative to the duration of the overall avoidance or recovery maneuver. Hence, these maneuvers initially may be treated as instantaneous maneuvers. Having defined the desired instantaneous maneuvers, the acceleration / turn rate constraint maneuvers are derived. This is analogous to determining the desired guidance command and using this guidance command to derive the corresponding control command.

Also it is assumed that the aircraft state is known perfectly and the state propagation is assumed to occur without error. Finally, in this report, the focus is on the maneuvers performed by one aircraft; however, the equations are general enough to handle the case where either of both aircraft perform the conflict resolution maneuvers.

1.2 Results

For the scenarios that were investigated, the time to loss of separation with an intruder or hazard was set at about 5 minutes. Hence, under this tactical scenario where the aircraft were at a typical cruise altitude of FL310, it was determined that the speed-only maneuvers were generally infeasible. This arose from the fact that the required speeds exceeded either the maximum thrust speed limit or the minimum buffet speed limit.

On the other hand, the track angle-only avoidance and recovery maneuvers were generally feasible even when an operationally acceptable maneuver limit of ±60 degrees was imposed. The track angle only maneuvers also achieved the highest efficiency metric relative to maneuvers that consisted of combined speed and track angle maneuvers.

While the combined speed and track angle avoidance maneuvers are not unique, this report focused on an optimum combination of these maneuvers. Taken from [1], the optimal maneuver was defined as the avoidance maneuver that requires the smallest change in the own aircraft velocity (speed and track angle) vector. In the case that the speed avoidance maneuver for this optimum maneuver exceeds a limit, the speed is reset to the nearest limit. Then a corresponding track angle maneuver is selected that will still lead to an avoidance of the intruder. If the recovery speed maneuver limit is exceeded there is no alternative but to declare this optimum (or sub-optimum) avoidance and recovery maneuver to be infeasible.

For the parametric crossing angle cases, the crossing angle of the intruder aircraft relative to the own aircraft was varied in increments of ten degrees. For all the maneuver test cases investigated in this report, the conflict was constructed in such a way that if no avoidance maneuver was used, the own aircraft would not only penetrate the protected zone around an intruder but also collide with the intruder. As a result, the own aircraft always had a choice of performing an avoidance maneuver that led the own aircraft to pass ahead or behind the intruder aircraft. With the efficiency metric, it was then possible to see which of these two maneuvers produced the highest efficiency.

For the parametric crossing angle cases, it was found that for the small crossing angle cases of ±20 deg or so, the avoidance maneuvers were found to be infeasible. This arises from the fact that the relative avoidance velocity between the own and intruder aircraft is very low. As a result, any maneuver that further reduced this relative avoidance velocity generally resulted in excessively long avoidance maneuver times. Hence, the own aircraft ended up passing its next waypoint before being able to initiate its

recovery maneuver. Therefore, these avoidance maneuvers were also considered to be impractical.

1.3 Further Work

Work in this report focused exclusively on the planar conflict detection and resolution problem. As a result, only speed, track angle, or a combination of these maneuvers was investigated. Because of the vertical dimension of the real-world CD&R problem, future work should extend the current analysis to include vertical conflict avoidance and recovery maneuvers. This is especially relevant to conflicts involving climbing or descending aircraft. The own aircraft would then be able to add an altitude change to the maneuver options that it could exploit, in addition to the speed and track angle maneuvers. The efficiency metric could be extended, as necessary, to evaluate the merits of these altitude maneuvers as well.

This report also addressed the CD&R problem when there is perfect knowledge of the own and intruder aircraft position and velocity. When the uncertainties in this knowledge are considered and the conflicts are detected at longer (strategic) ranges, the decision arises of when to initiate the avoidance maneuver. If the maneuver is initiated as soon as the conflict is detected, the uncertainty in the knowledge of the states of the intruder aircraft is largest. Hence, an avoidance maneuver may be selected that is not optimum or may not actually be necessary. On the other hand, if the maneuver is delayed to reduce the uncertainty in the intruder aircraft state, a larger and less efficient maneuver may be required. Hence, it is recommended to explore this trade-off using the efficiency metric to determine the best avoidance maneuver option.

2 Introduction

This report presents conflict detection, avoidance, and recovery algorithms in the horizontal plane when an intruder aircraft threatens the safety of the own aircraft. In addition avoidance of stationary hazards, such as terrain or special use airspace (SUA) or moving hazards, such as storm cells is investigated. The recovery phase requires that the own aircraft turns back to its original flight plan. This requires the aircraft to fly to its next waypoint. If it was originally in a miles-in-trail (MIT) slot, it must return to its MIT slot. Returning back to the next waypoint may also be required with a recovery a recovery velocity to satisfy a required time of arrival (RTA) constraint at the next waypoint. The general scenarios are illustrated in Figure 1.

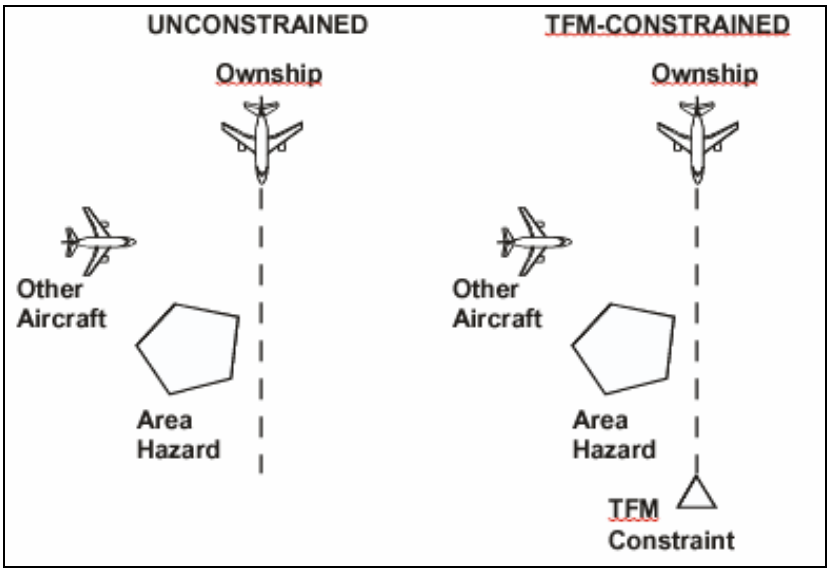

Figure 1. Aircraft Conflict Scenarios

The avoidance maneuvers that are examined include speed, track angle, or a combination of both. Once the avoidance maneuvers have been selected, the requirement that the own aircraft return back to its original flight plan dictates the required recovery maneuver, whether speed, track angle, or a combination of these two maneuvers.

The avoidance and recovery maneuvers are initially assumed to be achieved instantaneously. After the avoidance and recovery maneuvers have been identified, acceleration/turn rate-limited avoidance and recovery maneuvers are presented. In addition, the speed maneuver envelope for a typical aircraft, the MD-80, is investigated. This maneuver envelope is used to determine the available speed limits at cruise altitude. In addition, the maximum acceleration, deceleration, and turn rates that this aircraft can achieve at cruise altitude are identified.

To provide a comparison between alternate conflict resolution maneuvers, a performance metric is developed. This so-called efficiency metric (EM) incorporates the direct operating cost (DOC) of the own aircraft. The DOC is based on the flight time and expended fuel costs. The EM starts by computing the nominal DOC between the current location of the aircraft and the next waypoint. It then compares the nominal DOC to the DOC that is required to perform the conflict avoidance and recovery to the next waypoint.

Following the theoretical developments, a set of single crossing angle cases are evaluated. The single crossing angle cases assume that the intruder aircraft will produce a broadside (-90 deg crossing angle) conflict with the own aircraft if no evasive maneuvers are taken. In addition, conflict with a stationary hazard directly in front of the own aircraft or a moving hazard that moves across the nominal flight path of the own aircraft is investigated.

Following the single crossing angle encounter cases, a number of parametric crossing angle cases are investigated. These cases also include situations where the own aircraft initial speed is 10% faster or 10% slower than the intruder aircraft.

In this report, the focus is on analytic or semi-analytic algorithms that describe the conflict detection, avoidance, and recovery phases of flight. This report also draws on work previously reported by other authors and extends this work, where relevant.

3 Two-Aircraft Conflict Detection and Avoidance

3.1 Conflict Detection:

To introduce the nomenclature that will be used in this paper, the conflict avoidance problem between two aircraft is summarized and illustrated in Figure 2 in a local-level coordinate system. In Figure 3 it is also presented in an intruder aircraft-centered local-level coordinate system. Key variables are further illustrated in Figure 4 that shows a potential conflict of the own (O) aircraft with an intruder (I) aircraft in the relative coordinate system.

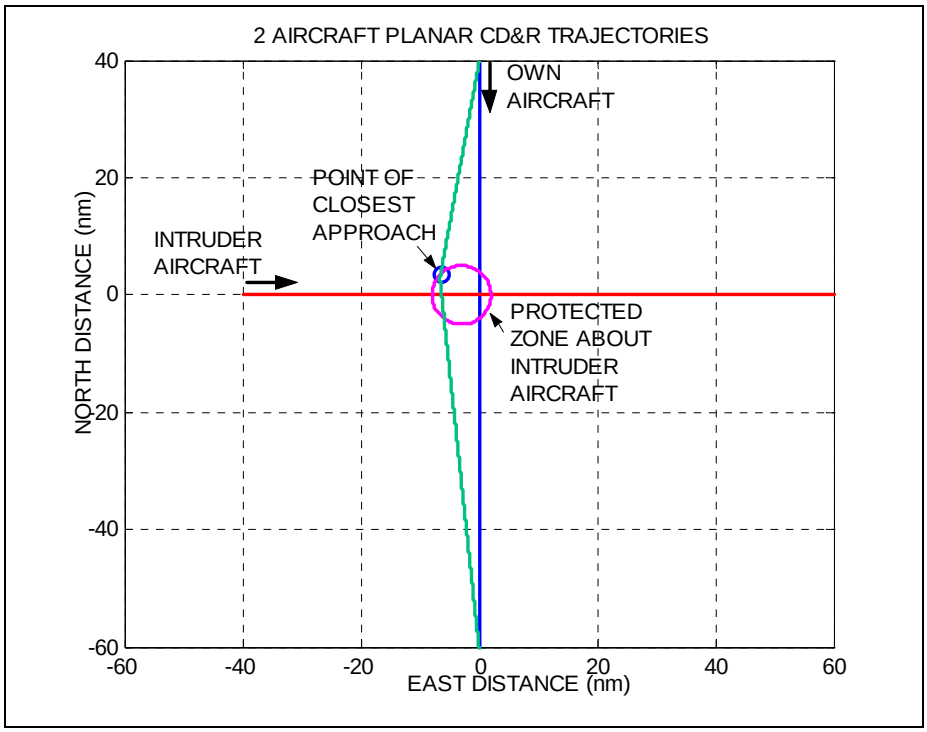

Figure 2. Two Aircraft Conflict Avoidance Scenario with Recovery to Fixed Waypoint
(Local-level coordinates, Own aircraft uses track angle maneuvers to pass behind intruder)

A circular protected region about the intruder aircraft of radius R_p is defined. Using this protected zone, a conflict may occur (is detected) when the own aircraft is moving toward the intruder aircraft:

$$\dot{R} \le 0 \qquad \text{and,} \quad s_C < R_P \tag{1}$$

The separation distance, s_C, at the point of closest approach is:

$$s_C = R \sin\left(\beta - 180^0\right) \tag{2}$$

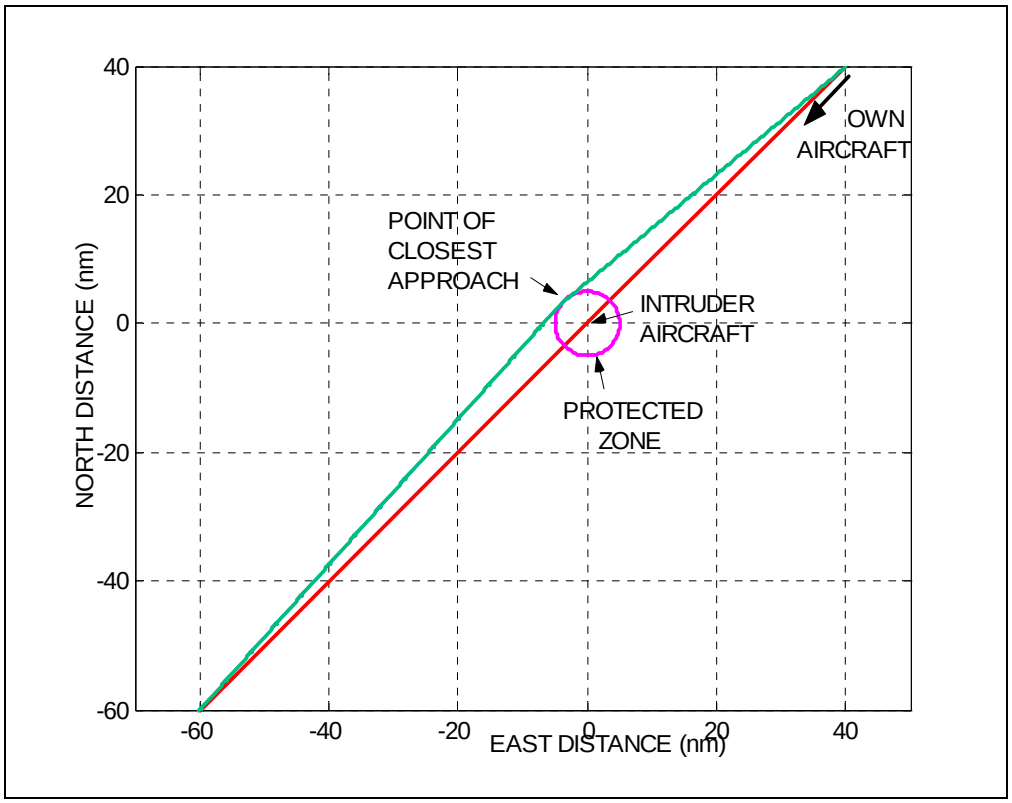

Figure 3. Two Aircraft Conflict Avoidance Scenario with Recovery to Fixed Waypoint
(Intruder-centered Coordinates, Own aircraft uses track angle maneuvers to pass behind intruder)

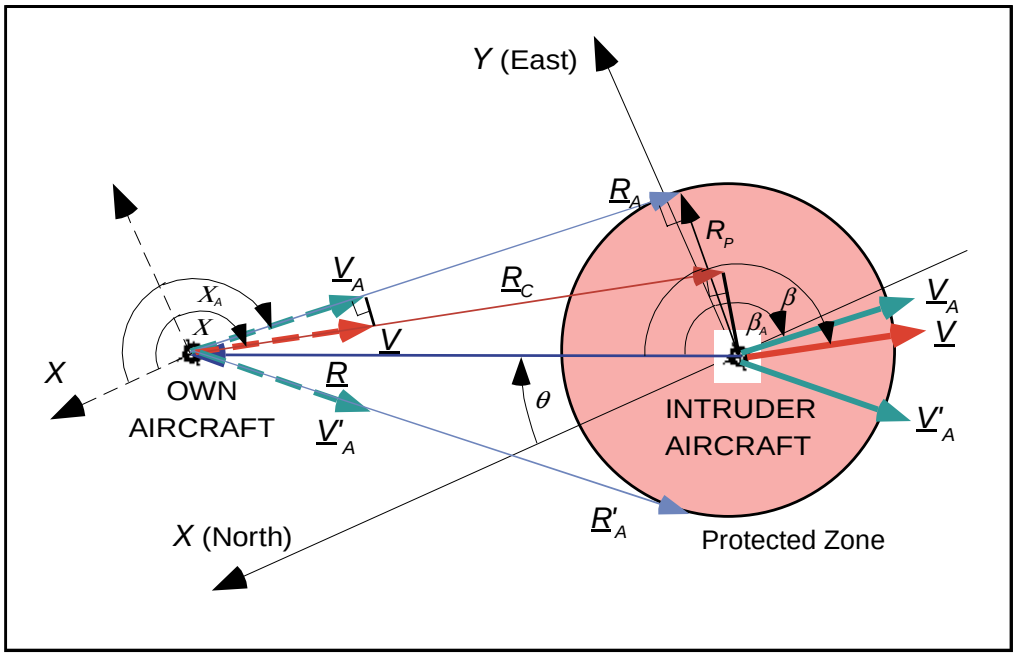

Figure 4. Illustration of Variables Required for Conflict Detection and Avoidance
(Intruder Aircraft-centered Coordinates)

The range rate: $$\dot{R} = V\cos\beta \tag{3}$$

The relative track angle is: $$\beta \equiv (\mathrm{X} - \theta) \tag{4}$$

The relative velocity track angle is:

$$\mathrm{X} = \arctan\left(\frac{v_O \sin\chi_O - v_I \sin\chi_I}{v_O \cos\chi_O - v_I \cos\chi_I}\right) \tag{5}$$

The relative range azimuth angle is:

$$\theta = \arctan\left(\frac{y_O - y_I}{x_O - x_I}\right) \tag{6}$$

3.2 Conflict Avoidance

This section summarizes the two-aircraft avoidance maneuvers as developed in [1]. For the scenario illustrated in Figure 4, the conflict is avoided by changing the relative track angle, β, to β_A:

$$\beta_A = 180^0 \pm \arcsin\left(\frac{R_P}{R}\right) \tag{7}$$

Of the two solutions in (7), the solution that requires the smallest change from β, to β_A is usually chosen. If this change is of the same magnitude for maneuvers to the left or right, other factors may be considered. These factors include selecting the maneuver that is achieved with the highest performance using the efficiency metric (EM) that will be presented later.

The avoidance relative velocity track angle based on (5) - (7) is:

$$\mathrm{X}_A = (\theta + \beta_A) = \arctan\left(\frac{v_{OA} \sin\chi_{OA} - v_{IA} \sin\chi_{IA}}{v_{OA} \cos\chi_{OA} - v_{IA} \cos\chi_{IA}}\right) \tag{8}$$

In (8), the unknown variables are the own aircraft avoidance speed and track angle, v_{OA} and χ_{OA}, and the intruder avoidance speed and track angle, v_{IA} and χ_{IA}. Hence, any combination of these four variables can be selected so long as they satisfy (8).

One strategy proposed in [1], partitions the required change in the relative track angle, $(\mathrm{X}_A - \mathrm{X})$, between the own aircraft and the intruder. Hence, if f_1 and f_2 is the fraction of the change in the relative track angle assigned to each aircraft. Then:

$$X_{A1} \equiv X + f_1 \cdot (X_A - X) \tag{9}$$

and,

$$X_{A2} \equiv X + f_2 \cdot (X_A - X) \tag{10}$$

where

$$f_1 + f_2 = 1 \tag{11}$$

Default values for $f_1 = f_2 = 0.5$, corresponding to a 50%-50% split between the two aircraft. Hence, using (8) together with either (9) and (10):

$$X_{A1} = \arctan\left(\frac{v_{OA}\sin\chi_{OA} - v_I \sin\chi_I}{v_{OA}\cos\chi_{OA} - v_I \cos\chi_I}\right) \tag{12}$$

and,

$$X_{A2} = \arctan\left(\frac{v_O \sin\chi_O - v_{IA}\sin\chi_{IA}}{v_O \cos\chi_O - v_{IA}\cos\chi_{IA}}\right) \tag{13}$$

If only the own aircraft speed or track angle is used to perform the avoidance maneuver, either a speed-only avoidance maneuver or a track angle-only avidance maneuver can be used [1]:

$$v_{OA} = v_I\left[\frac{\sin(X_A - \chi_I)}{\sin(X_A - \chi_O)}\right] \tag{14}$$

or,

$$\chi_{OA} = X_A - \arcsin\left\{\left(\frac{v_I}{v_O}\right)\sin(X_A - \chi_I)\right\} \tag{15}$$

Caution must be used to select the correct solution for the arcsine function in (15). This follows, since the arcsine has two possible solutions. Also, the argument of this function must not exceed a magnitude of 1.0.

As shown in [1], the geometric optimal (minimum required own aircraft velocity vector change) combined speed and track angle avoidance maneuvers are:

$$\chi_{OA} = X_A - \arctan\left[\frac{v_I \sin(X_A - \chi_I)}{v_O \sin(X_A - \chi_O)}\right] \tag{16}$$

and,

$$v_{OA} = v_O\left[\frac{\cos(X_A - \chi_O)}{\cos(X_A - \chi_{OA})}\right] \tag{17}$$

By reversing the role of own and intruder aircraft in (14) - (17), the corresponding optimal dual avoidance maneuvers for the intruder aircraft are obtained.

4 Aircraft Recovery

4.1 Recovery to Moving Waypoint (Miles in Trail Constraint)

While waypoints in general are stationary, moving waypoints arise when an aircraft must reach a miles-in-trail (MIT) slot in a stream of traffic. This case is illustrated in Figure 5 in a local-level coordinate system and in Figure 6 in an intruder-centered local level coordinate system.

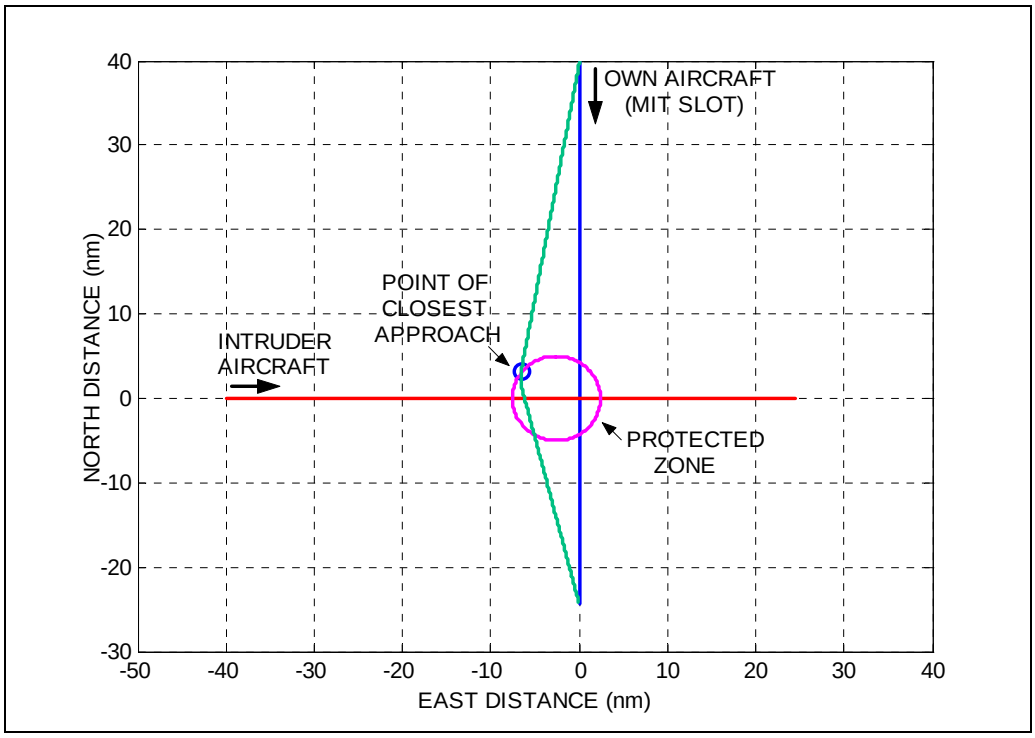

Figure 5. 2-Aircraft CD&R Maneuvers
(Local Level Coordinates, MIT Constraint)

The conflict recovery maneuver nominally is initiated when the conflict avoidance maneuver has been completed. The avoidance maneuver is completed when the own aircraft reaches the point of closest approach (PCA) to the intruder aircraft. The nominal coordinates of the point of closest approach to the intruder aircraft, relative to the point at which the conflict was detected, is obtained using the time to reach the point of closest approach, t_{PCA}:

$$\begin{pmatrix} x_{O,PCA} \\ y_{O,PCA} \end{pmatrix} = \begin{pmatrix} x_O \\ y_O \end{pmatrix} + t_{PCA} v_{OA} \begin{pmatrix} \cos\chi_{OA} \\ \sin\chi_{OA} \end{pmatrix} \tag{18}$$

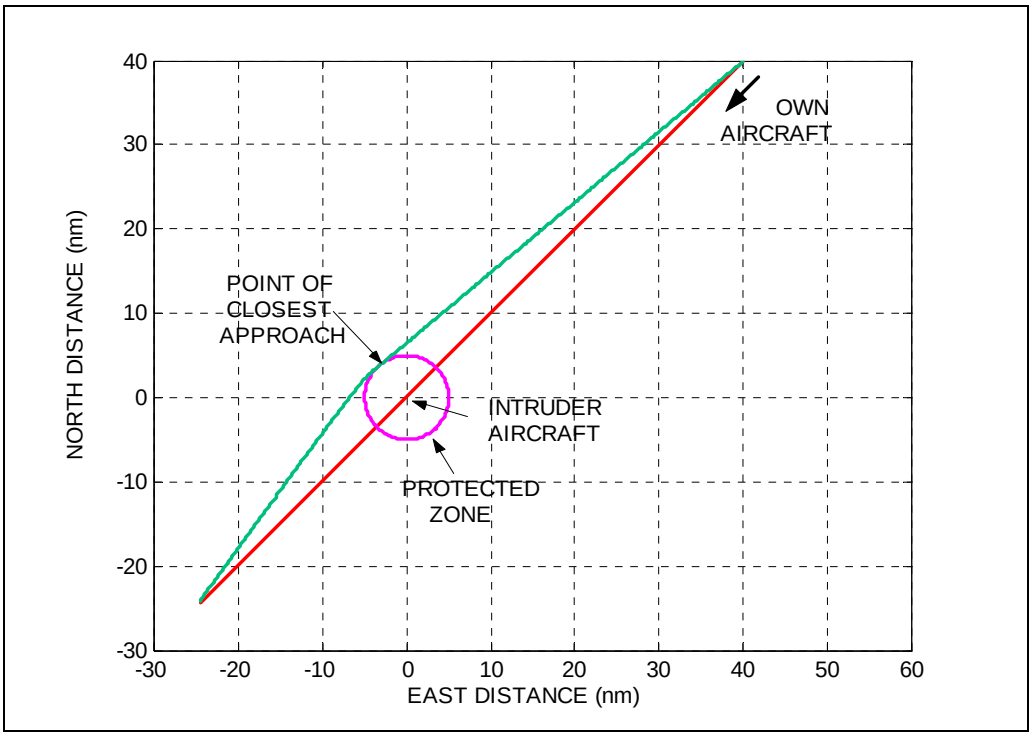

Figure 6. 2 Aircraft CD&R Maneuvers
(Intruder-centered Coordinates, MIT Constraint)

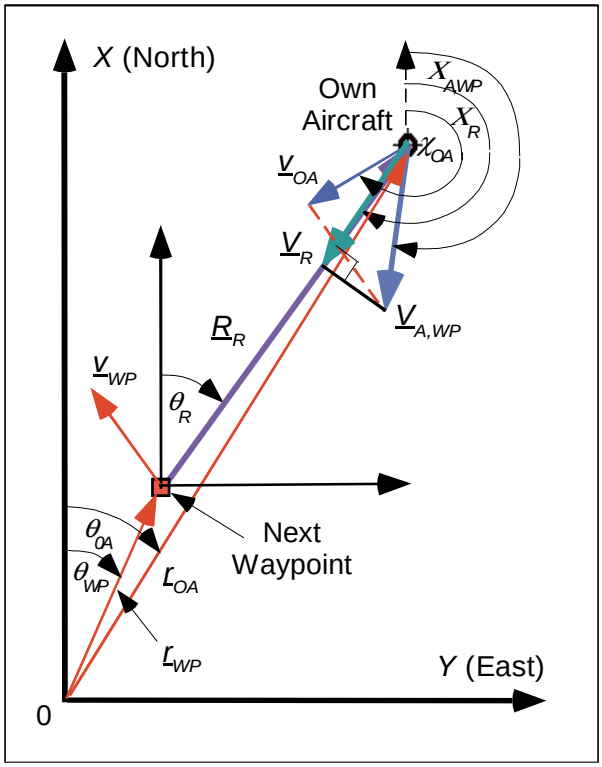

Figure 7. Recovery Geometry to Next Waypoint
(Local Level Coordinates)

where,

$$t_{PCA} = -\left(\frac{R\cos\beta_A}{V_A}\right) \tag{19}$$

The azimuth angle for the relative recovery range at the point of closest approach for the general case of a moving waypoint is:

$$\theta_{R,PCA} = \arctan\left(\frac{y_{O,PCA} - y_{WP,PCA}}{x_{O,PCA} - x_{WP,PCA}}\right) \tag{20}$$

where,

$$\begin{pmatrix} x_{WP,PCA} \\ y_{WP,PCA} \end{pmatrix} = \begin{pmatrix} x_{WP} \\ y_{WP} \end{pmatrix} + t_{PCA} v_{WP} \begin{pmatrix} \cos\chi_{WP} \\ \sin\chi_{WP} \end{pmatrix} \tag{21}$$

The recovery problem is similar to the two aircraft conflict avoidance problem in the last section. Hence, a necessary and sufficient condition for recovery to the moving waypoint is for the relative velocity track angle, X_R, to be aligned with the relative range azimuth angle, θ_R, in (20):

$$X_{R,PCA} = \left(\theta_{R,PCA} + 180^0\right) \tag{22}$$

Before this recovery maneuver is executed, it must be checked to see that it does not violate the protected region around the intruder aircraft, as illustrated in Figure 8.

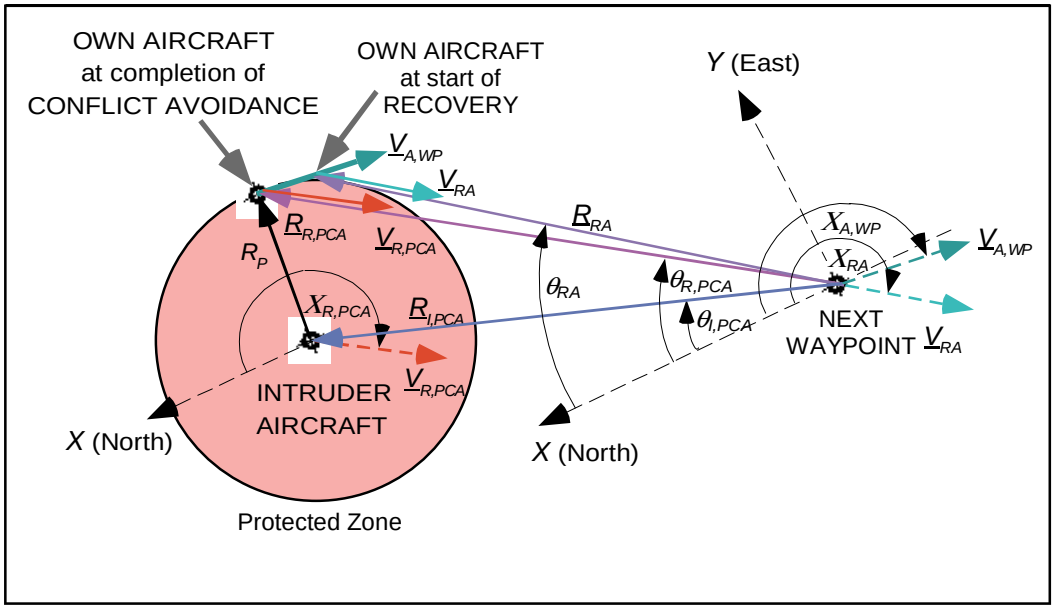

Figure 8. Conflict-Free Recovery Geometry
(Waypoint-centered Local Level Coordinates)

Using the circular protected region about the intruder aircraft of radius R_p, a conflict may occur (is detected) when the own aircraft is moving toward the intruder aircraft if:

$$s_{C,R} < R_P \tag{23}$$

The recovery minimum separation distance, $s_{C,R}$, at the point of closest approach is:

$$s_{C,R} = R_{WP,PCA} \sin\left(\mathrm{X}_{R,PCA} - \theta_{WP,PCA} - 180^0\right) \tag{24}$$

If (23) is not satisfied, then the recovery maneuver is initiated at:

$$t_A = t_{PCA} \tag{25}$$

If (23) is satisfied, the recovery maneuver cannot be initiated at the completion of the avoidance maneuver as specified by (19). Instead, it must be delayed by small time interval, Δt_A:

$$\Delta t_A = \frac{\left(R_P - s_{C,R}\right)}{\dot{s}_{C,R}} \tag{26}$$

This leads to a total avoidance maneuver time of:

$$t_A = t_{PCA} + \Delta t_A \tag{27}$$

Rather than try to solve (26), the most convenient way to determine this delay is to perform a simple numerical search for the minimum delay that will avoid a recovery conflict. Hence, a search is started with a 1-second delay and is incremented by 1 second until the minimum necessary delay is obtained.

The new location for the start of the recovery maneuver is then:

$$\begin{pmatrix} x_{OA} \\ y_{OA} \end{pmatrix} = \begin{pmatrix} x_O \\ y_O \end{pmatrix} + t_A v_{OA} \begin{pmatrix} \cos\chi_{OA} \\ \sin\chi_{OA} \end{pmatrix} \tag{28}$$

With this time delay and the scenario illustrated in Figure 7, the conflict is avoided and recovery to the MIT slot is initiated by changing the avoidance relative velocity track angle, $\mathrm{X}_{A,WP}$, to X_{RA}:

$$\mathrm{X}_{RA} = \theta_{WP,A} + 180^0 \pm \arcsin\left(\frac{R_P}{R_{WP,A}}\right) \tag{29}$$

where,

$$\mathrm{X}_{A,WP} = \arctan\left(\frac{v_{OA}\sin\chi_{OA} - v_{WP}\sin\chi_{WP}}{v_{OA}\cos\chi_{OA} - v_{WP}\cos\chi_{WP}}\right) \tag{30}$$

$$\theta_{WP,A} = \arctan\left(\frac{y_{IA} - y_{WP,A}}{x_{IA} - x_{WP,A}}\right) \tag{31}$$

$$R_{WP,A} = \sqrt{\left[x_{IA} - x_{WP,A}\right]^2 + \left[y_{IA} - y_{WP,A}\right]^2} \tag{32}$$

$$\begin{pmatrix} x_{WP,A} \\ y_{WP,A} \end{pmatrix} = \begin{pmatrix} x_{WP} \\ y_{WP} \end{pmatrix} + t_A v_{WP} \begin{pmatrix} \cos\chi_{WP} \\ \sin\chi_{WP} \end{pmatrix} \tag{33}$$

$$\begin{pmatrix} x_{IA} \\ y_{IA} \end{pmatrix} = \begin{pmatrix} x_{I} \\ y_{I} \end{pmatrix} + t_A v_{I} \begin{pmatrix} \cos\chi_{I} \\ \sin\chi_{I} \end{pmatrix} \tag{34}$$

The recovery relative velocity vector is:

$$\underline{V}_{RA} \equiv \begin{pmatrix} V_{RA}\cos\mathrm{X}_{RA} \\ V_{RA}\sin\mathrm{X}_{RA} \end{pmatrix} = \begin{pmatrix} v_{OR}\cos\chi_{OR} \\ v_{OR}\sin\chi_{OR} \end{pmatrix} - \begin{pmatrix} v_{WP}\cos\chi_{WP} \\ v_{WP}\sin\chi_{WP} \end{pmatrix} \tag{35}$$

The recovery relative velocity magnitude is:

$$V_{RA} = \sqrt{v_{OR}^2 - 2v_{OR}v_{WP}\cos\left(\chi_{OR} - \chi_{WP}\right) + v_{WP}^2} \tag{36}$$

The recovery relative track angle is:

$$\mathrm{X}_{RA} = \arctan\left(\frac{v_{OR}\sin\chi_{OR} - v_{WP}\sin\chi_{WP}}{v_{OR}\cos\chi_{OR} - v_{WP}\cos\chi_{WP}}\right) \tag{37}$$

With the relative recovery track angle, X_{RA}, given by (29), the unknown variables in (37) are the recovery speed and track angle, v_{OR} and χ_{OR}.

With (35) the following constraint equations are obtained:

$$v_{OR}\sin\chi_{OR} = V_{RA}\sin\mathrm{X}_{RA} + v_{WP}\sin\chi_{WP} \tag{38}$$

and,

$$v_{OR}\cos\chi_{OR} = V_{RA}\cos\mathrm{X}_{RA} + v_{WP}\cos\chi_{WP} \tag{39}$$

Using (38) and (39), the recovery maneuver speed and track angle, v_{OR} and χ_{OR} are:

$$v_{OR} = \sqrt{V_{RA}^2 + 2v_{WP}V_{RA}\cos(\mathrm{X}_{RA} - \chi_{WP}) + v_{WP}^2} \tag{40}$$

and,

$$\chi_{OR} = \arctan\left[\frac{V_{RA}\sin\mathrm{X}_{RA} + v_{WP}\sin\chi_{WP}}{V_{RA}\cos\mathrm{X}_{RA} + v_{WP}\cos\chi_{WP}}\right] \tag{41}$$

The choice of the recovery relative velocity magnitude, V_{RA}, is arbitrary and only determines the time required to complete the recovery maneuver, t_R. An appropriate choice for V_{RA} is based on the desired time to return to the miles-in-trail slot:

$$t_R = \frac{R_{RA}}{V_{RA}} \tag{42}$$

where,

$$\begin{aligned} R_{RA} = \Big[&\big((x_O - x_{WP}) + t_A(v_{OA}\cos\chi_{OA} - v_{WP}\cos\chi_{WP})\big)^2 \\ &+ \big((y_O - y_{WP}) + t_A(v_{OA}\sin\chi_{OA} - v_{WP}\sin\chi_{WP})\big)^2\Big]^{0.5} \end{aligned} \tag{43}$$

An appropriate choice for V_{RA} is based on selecting the fastest time for the aircraft to return to its miles-in-trail slot. Hence based on (40), V_{RA} is selected such that the maximum aircraft speed, $v_{OR,MAX}$, is used:

$$V_{RA} = -v_{WP}\cos(\mathrm{X}_{RA} - \chi_{WP}) + \sqrt{v_{OR,MAX}^2 - v_{WP}^2\sin^2(\mathrm{X}_{RA} - \chi_{WP})} \tag{44}$$

Using (44) in (40) and (41) yields the recovery maneuver with the shortest feasible recovery time.

4.2 Recovery to Fixed Waypoint

For the special case where the waypoint is stationary $(v_{WP} = 0)$, the recovery speed, v_{OR}, is unconstrained (arbitrary) and can be reset to the nominal cruise speed, v_O. The recovery track angle specified in (41) and using (29) simplifies to:

$$\chi_{OR} = (\theta_{RA} + 180^0) \tag{45}$$

where,

$$\theta_{RA} = \arctan\left(\frac{y_{OA} - y_{WP}}{x_{OA} - x_{WP}}\right) \tag{46}$$

4.3 Recovery to Fixed Waypoint (Required Time of Arrival Constraint)

The recovery track angle is defined by (45). The equation for the recovery speed based on [2] is:

$$v_{OR} = \frac{\sqrt{\rho_{WP}^2 - 2\rho_{WP}\rho_A \cos(\chi_{OA} - \chi_O) + \rho_A^2}}{\left(\frac{\rho_{WP}}{v_O}\right) - \left(\frac{\rho_A}{v_{OA}}\right)} \tag{47}$$

where

$$\rho_A = \sqrt{(x_{OA} - x_O)^2 + (y_{OA} - y_O)^2} \tag{48}$$

$$\rho_R = \sqrt{(x_{OA} - x_{WP})^2 + (y_{OA} - y_{WP})^2} \tag{49}$$

$$\rho_{WP} = \sqrt{(x_O - x_{WP})^2 + (y_O - y_{WP})^2} \tag{50}$$

4.4 Post-Recovery Maneuver

When the own aircraft intercepts its MIT slot, it must perform a final (post-recovery) maneuver. This maneuver adjusts the own aircraft to the MIT slot speed and track angle in order that the aircraft remains within this slot.

5 Area Hazards

While Section 3 focused on the problem of the own aircraft avoiding an intruder aircraft, this section addresses the problem of the own aircraft avoiding an extended (area) hazard. The area hazards may consist of stationary hazards, such as special use airspace or terrain. Alternately the area hazards may be moving, such as a thunder storm.

When dealing with area hazards, a region must be avoided that cannot be described simply as the circular protected region around an intruder. Hence, a more general search must be made to determine the minimum and maximum relative range azimuth angles, θ_{Hi}, between the hazard area and the own aircraft. These azimuth angles are based on the nodes, (x_{Hi}, y_{Hi}) that define an area that is moving with a velocity (v_H, χ_H) as illustrated in Figure 9 and 10.

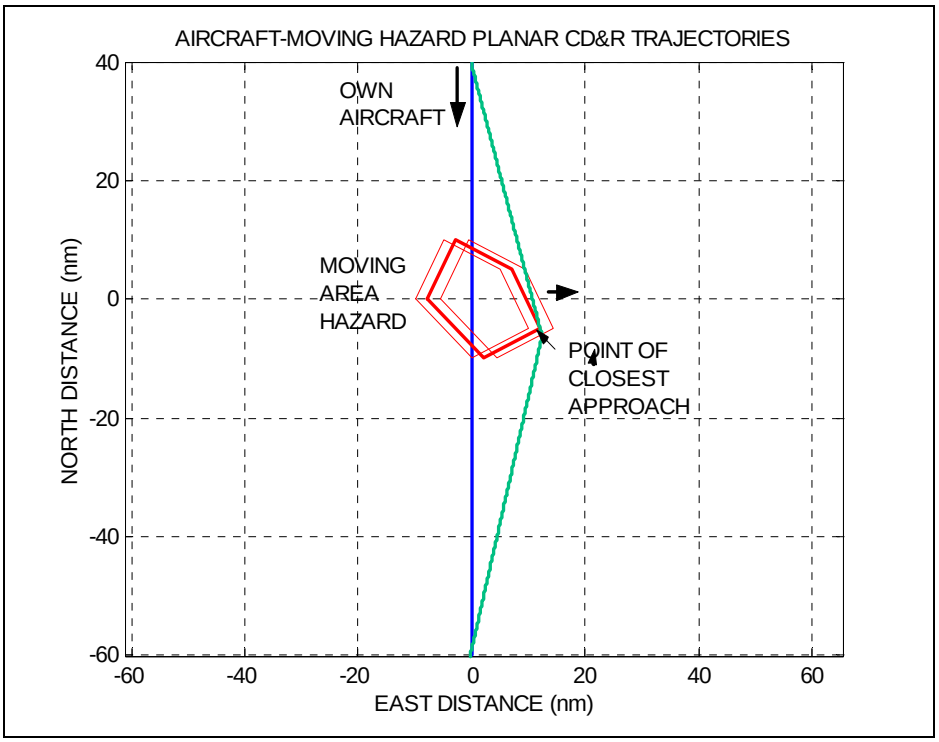

Figure 9. Aircraft-Moving Hazard Avoidance Scenario with Recovery to Fixed Waypoint (Local Level Coordinates; Aircraft passes ahead of hazard without a maneuver buffer)

Key parameters for this problem are presented in Figure 11. Whether a conflict with the area hazard is possible is determined based on the current relative geometry and speed. For detection, the minimum and maximum range angle for all the range angles, θ_{Hi}, corresponding to *i* nodes describing the area hazard must be found:

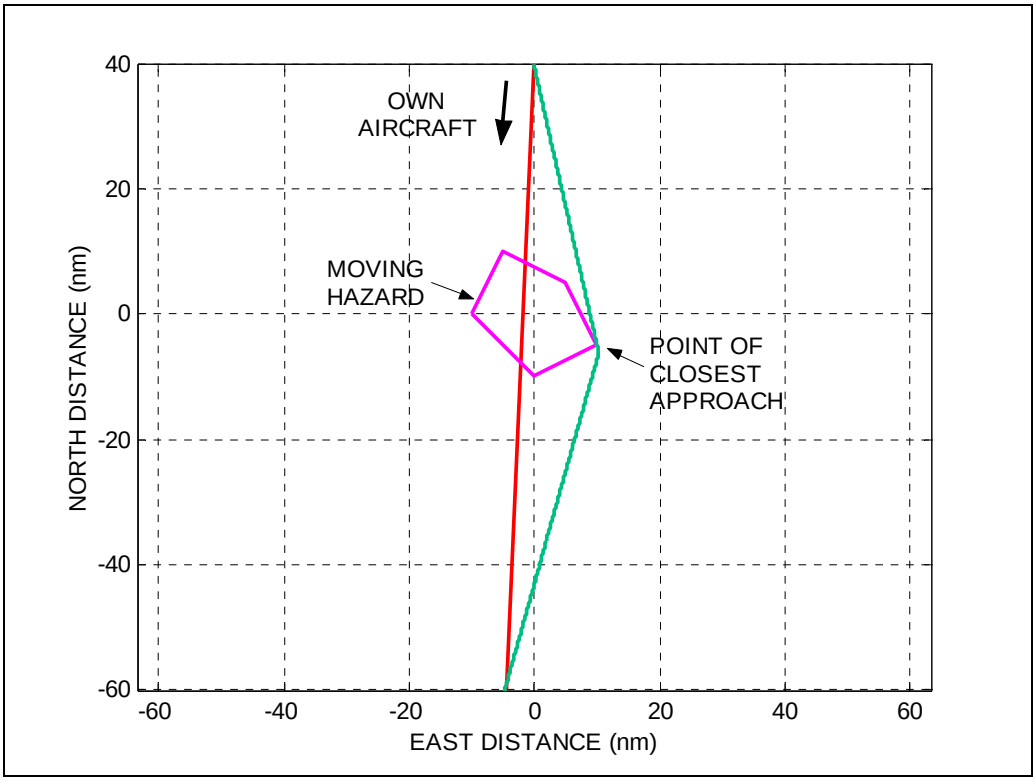

Figure 10. Aircraft-Moving Hazard Avoidance Scenario with Recovery to Fixed Waypoint (Hazard-centered Coordinates; Aircraft passes ahead of hazard without a maneuver buffer)

$$\theta_{MIN} \equiv Min\{\theta_{H1},\cdots,\theta_{Hn}\} \tag{51}$$

and,

$$\theta_{MAX} \equiv Max\{\theta_{H1},\cdots,\theta_{Hn}\} \tag{52}$$

The relative range azimuth angle is:

$$\theta_{Hi} = \arctan\left(\frac{y_O - y_{Hi}}{x_O - x_{Hi}}\right) \tag{53}$$

A conflict with the area hazard is possible if:

$$\theta_{MIN} < \left(\chi_O - 180^0\right) < \theta_{MAX} \tag{53}$$

Now the relative velocity, $\underline{V}$, between the own aircraft and the area hazard:

$$\underline{V} \equiv \begin{pmatrix} V\cos \mathrm{X} \\ V\sin \mathrm{X} \end{pmatrix} = \begin{pmatrix} v_O \cos\chi_O - v_H \cos\chi_H \\ v_O \sin\chi_O - v_H \sin\chi_H \end{pmatrix} \tag{54}$$

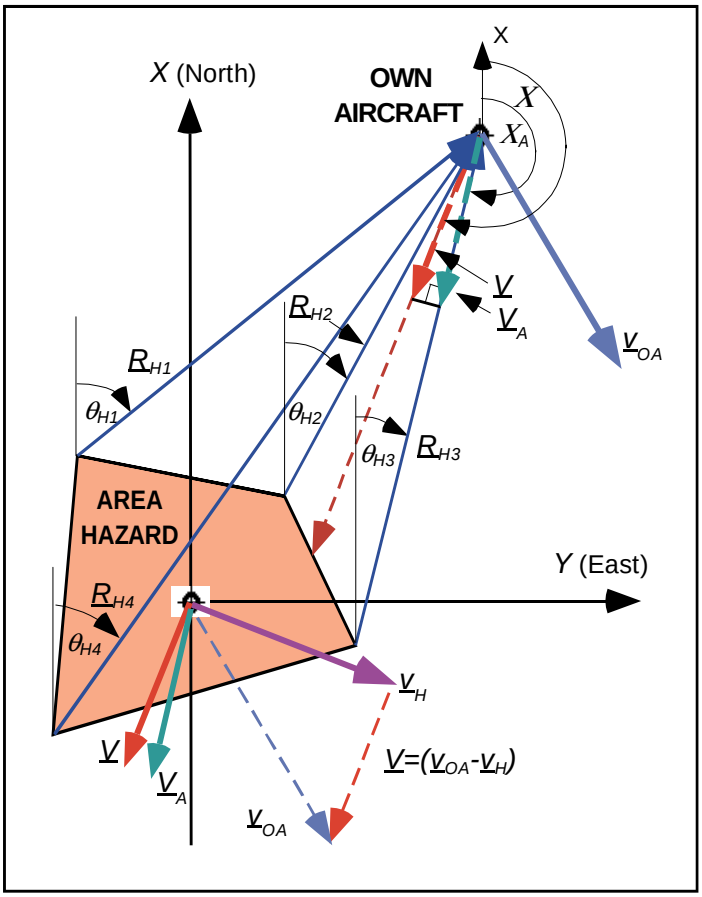

Figure 11. Encounter Geometry with a Moving Area Hazard
(Hazard-centered Coordinates)

The relative velocity track angle is:

$$\mathrm{X} = \arctan\left(\frac{v_O \sin\chi_O - v_H \sin\chi_H}{v_O \cos\chi_O - v_H \cos\chi_H}\right) \tag{55}$$

Hence the relative avoidance maneuver velocity vector around the moving area hazard:

$$\underline{V}_A \equiv \begin{pmatrix} V_A \cos \mathrm{X}_A \\ V_A \sin \mathrm{X}_A \end{pmatrix} = \begin{pmatrix} v_{OA} \cos\chi_{OA} - v_H \cos\chi_H \\ v_{OA} \sin\chi_{OA} - v_H \sin\chi_H \end{pmatrix} \tag{56}$$

The relative avoidance velocity track angle is:

$$\mathrm{X}_A = \arctan\left(\frac{v_{OA} \sin\chi_{OA} - v_H \sin\chi_H}{v_{OA} \cos\chi_{OA} - v_H \cos\chi_H}\right) \tag{57}$$

The relative avoidance velocity track angle must satisfy:

$$\mathrm{X}_A = \left(\theta_{MIN} - \Delta\theta_{B,MIN} + 180^0\right) \tag{58}$$

or,

$$\mathrm{X}_A = \left(\theta_{MAX} + \Delta\theta_{B,MAX} + 180^0\right) \tag{59}$$

The avoidance buffer around the hazard is defined by:

$$\Delta\theta_{B,MIN} \equiv \arctan\left(\frac{R_P}{R_{MIN}}\right) \tag{60}$$

and,

$$\Delta\theta_{B,MAX} \equiv \arctan\left(\frac{R_P}{R_{MAX}}\right) \tag{61}$$

The relative range values, R_{MIN} and R_{MAX}, correspond respectively to the conflict avoidance azimuth angles, θ_{MIN} and θ_{MAX}. The buffer, R_P (5 nm), is the protected radius that was introduced previously for the two-aircraft conflict avoidance problem [3]. Alternately, if the hazard consists of a severe weather region that may produce icing conditions on the aircraft, this buffer may be increased to four times (20 nm) the nominal protected radius [3].

The choice between (58) and (59) is usually made by selecting the angle that minimizes the change from X to X_A. If either choice requires the same magnitude of change, the maneuver efficiency metric, to be defined in a later section, can be used to select the preferred maneuver direction.

In (58) and (59), the minimum and maximum relative range azimuth angles and their corresponding buffer angles are calculated at the time of conflict detection for a moving hazard.

Now from Section 2, the same avoidance maneuver options that were developed for avoidance of a moving intruder aircraft can be applied to the avoidance of a moving hazard. Hence, if the own aircraft performs a single speed or track angle maneuver:

$$v_{OA} = v_H\left[\frac{\sin\left(\mathrm{X}_A - \chi_H\right)}{\sin\left(\mathrm{X}_A - \chi_O\right)}\right] \tag{62}$$

or,

$$\chi_{OA} = \mathrm{X}_A - \arcsin\left\{\left(\frac{v_H}{v_O}\right)\sin\left(\mathrm{X}_A - \chi_H\right)\right\} \tag{63}$$

Alternately, if the own aircraft performs a optimum speed and track angle avoidance maneuver:

$$\chi_{OA} = \mathrm{X}_A - \arctan\left[\frac{v_H \sin(\mathrm{X}_A - \chi_H)}{v_O \sin(\mathrm{X}_A - \chi_O)}\right] \tag{64}$$

and,

$$v_{OA} = v_O\left[\frac{\cos(\mathrm{X}_A - \chi_O)}{\cos(\mathrm{X}_A - \chi_{OA})}\right] \tag{65}$$

Once the own aircraft has completed the avoidance maneuvers around either a stationary or moving hazard, any of the recovery maneuvers of Section 4 can be selected.

6 Acceleration/Turn Rate Limited Maneuvers

6.1 General Avoidance Maneuver Problem

When performing a speed or track angle maneuver, a finite time is required to reach the desired speed or track angle. In the case of speed maneuvers, the maximum acceleration (or deceleration) determines how fast the desired speed maneuver value is reached. In the case of track angle maneuvers, the maximum turn rate determines how fast the desired track angle value is reached. Up to now, it has been assumed that the desired maneuver values can be reached nearly instantaneously. This is a reasonable assumption, if the time required to make the desired track angle change is small compared to the overall duration of the maneuver.

In the context of the last three sections, the discussion has focused on the guidance commands required to avoid an intruder aircraft followed by the guidance commands to recover to the next waypoint. In this section, the focus is on the control commands that will allow the desired guidance commands to be realized. Since the control system utilizes the finite acceleration and turn rate limits achievable by the maneuvering aircraft, it must select alternate avoidance and recovery maneuvers whose net effect is the same as if the maneuvers had been implemented instantaneously. A commanded maneuver must be selected such that the average maneuver value over the duration of the maneuver is the same as the desired instantaneous maneuver value.

Starting with the initial relative velocity:

$$\underline{V} = \begin{pmatrix} v_O \cos\chi_O - v_{IA} \cos\chi_{IA} \\ v_O \sin\chi_O - v_{IA} \sin\chi_{IA} \end{pmatrix} \tag{66}$$

To avoid the intruder, the own aircraft has to change its speed and track angle such that the avoidance relative velocity is achieved:

$$\underline{V}_A = \begin{pmatrix} v_{OA} \cos\chi_{OA} - v_{IA} \cos\chi_{IA} \\ v_{OA} \sin\chi_{OA} - v_{IA} \sin\chi_{IA} \end{pmatrix} \tag{67}$$

The own aircraft avoidance maneuver speed and track angle, v_{OA} and χ_{OA}, must satisfy:

$$\mathrm{X}_A = (\theta + \beta_A) = \arctan\left(\frac{v_{OA} \sin\chi_{OA} - v_I \sin\chi_I}{v_{OA} \cos\chi_{OA} - v_I \cos\chi_I} \right) \tag{68}$$

with,

$$\beta_A = 180^0 \pm \arcsin\left(\frac{R_P}{R}\right) \tag{69}$$

The relative velocity maneuver that is required to avoid the intruder aircraft is:

$$\Delta\underline{V}_A \equiv \left(\underline{V}_A - \underline{V}\right) = \underline{v}_{OA} = \begin{pmatrix} v_{OA}\cos\chi_{OA} - v_O\cos\chi_O \\ v_{OA}\sin\chi_{OA} - v_O\sin\chi_O \end{pmatrix} \tag{70}$$

This relative velocity maneuver has to be made instantaneously and maintained for duration of the avoidance maneuver time, t_A:

$$\int_0^{t_A} \Delta\underline{V}_A dt = \begin{pmatrix} t_A v_{OA}\cos\chi_{OA} - t_A v_O\cos\chi_O \\ t_A v_{OA}\sin\chi_{OA} - t_A v_O\sin\chi_O \end{pmatrix} \tag{71}$$

If the relative velocity maneuver cannot be achieved instantaneously, then the time integral of the relative velocity maneuver must be remain unchanged when finite own aircraft speed and track angle maneuver changes are made:

$$\int_0^{t_A} \Delta\underline{V}_A dt = \int_0^{t_A} \begin{pmatrix} v_O(t)\cos\chi_O(t) - v_O\cos\chi_O \\ v_O(t)\sin\chi_O(t) - v_O\sin\chi_O \end{pmatrix} dt = \begin{pmatrix} t_A v_{OA}\cos\chi_{OA} - t_A v_O\cos\chi_O \\ t_A v_{OA}\sin\chi_{OA} - t_A v_O\sin\chi_O \end{pmatrix} \tag{72}$$

Now if the maximum change in speed is an acceleration (deceleration), a_O, then:

$$v_O(t) = v_O + \begin{cases} a_O t, & \text{if } t \le t_v \\ \Delta v_{OAC}, & \text{if } t > t_v \end{cases} \tag{73}$$

In (73), Δv_{OAC}, is the commanded speed change:

$$\Delta v_{OAC} \equiv \left(v_{OAC} - v_O\right) \tag{74}$$

Also, t_v, is the time required to achieve this speed change:

$$t_v = \left(\frac{\Delta v_{OAC}}{a_O}\right) \tag{75}$$

Likewise, if the maximum change in track angle is a turn rate, ω_O, then:

$$\chi_O(t) = \chi_O + \begin{cases} \omega_O t, \text{ if } t \le t_\chi \\ \Delta\chi_{OAC}, \text{ if } t > t_\chi \end{cases} \tag{76}$$

Similarly, in (76), $\Delta\chi_{OAC}$, is the commanded track angle change:

$$\chi_{OAC} \equiv (\chi_{OAC} - \chi_O) \tag{77}$$

Also, t_χ, is the time required to achieve this track angle change:

$$t_\chi = \left(\frac{\Delta\chi_{OAC}}{\omega_O} \right) \tag{78}$$

6.2 Avoidance Maneuver Linearity Approximation

If the change in track angle, $\Delta\chi_{OAC}$, is small, then (72) can be simplified using a 1st order Taylor series expansion of the sine and cosine functions of the track angles:

$$\int_0^{t_A} \Delta\underline{V}_A dt = \int_0^{t_A} \begin{pmatrix} \Delta v_O(t)\cos\chi_O - v_O\Delta\chi_O(t)\sin\chi_O \\ \Delta v_O(t)\sin\chi_O + v_O\Delta\chi_O(t)\cos\chi_O \end{pmatrix} dt = \begin{pmatrix} t_A\Delta v_{OA}\cos\chi_O - t_A v_O\Delta\chi_{OA}\sin\chi_O \\ t_A\Delta v_{OA}\sin\chi_O + t_A v_O\Delta\chi_{OA}\cos\chi_O \end{pmatrix} \tag{79}$$

where,

$$\Delta v_O(t) = \begin{cases} a_O t, \text{ if } t \le t_v \\ \Delta v_{OAC}, \text{ if } t > t_v \end{cases} \tag{80}$$

and,

$$\Delta\chi_O(t) = \begin{cases} \omega_O t, \text{ if } t \le t_\chi \\ \Delta\chi_{OAC}, \text{ if } t > t_\chi \end{cases} \tag{81}$$

When the track angle changes are too large to justify this 1st order Taylor series expansion, a 2nd order Taylor series expansion may be required. A 2nd order Taylor series expansion leads to a more complex set of coupled equations and hence is not recommended for practical considerations.

The components of the integral equality in (79):

$$\int_0^{t_A} \Delta v_O(t)\cos\chi_O dt - \int_0^{t_A} v_O\Delta\chi_O(t)\sin\chi_O dt = t_A(\Delta v_{OA}\cos\chi_O - v_O\Delta\chi_{OA}\sin\chi_O) \tag{82}$$

and,

$$\int_0^{t_A} \Delta v_O(t)\sin\chi_O dt + \int_0^{t_A} v_O \Delta\chi_O(t)\cos\chi_O dt = t_A(\Delta v_{OA}\sin\chi_O + v_O\Delta\chi_{OA}\cos\chi_O) \tag{83}$$

Substituting (80) and (81) into (82) and (83) and performing the integrations:

$$\begin{aligned}&\left[0.5a_O t_v^2 + (t_A - t_v)\Delta v_{OAC}\right]\cos\chi_O - \left[0.5\omega_O t_\chi^2 + (t_A - t_\chi)\Delta\chi_{OAC}\right]\cdot v_O\sin\chi_O \\ &= t_A(\Delta v_{OA}\cos\chi_O - v_O\Delta\chi_{OA}\sin\chi_O)\end{aligned} \tag{84}$$

and,

$$\begin{aligned}&\left[0.5a_O t_v^2 + (t_A - t_v)\Delta v_{OAC}\right]\sin\chi_O + \left[0.5\omega_O t_\chi^2 + (t_A - t_\chi)\Delta\chi_{OAC}\right]\cdot v_O\cos\chi_O \\ &= t_A(\Delta v_{OA}\sin\chi_O + v_O\Delta\chi_{OA}\cos\chi_O)\end{aligned} \tag{85}$$

Multiplying (84) by $\cos\chi_O$, (85) by $\sin\chi_O$, and adding the resulting equations together allows the velocity maneuver component to be isolated:

$$\left[0.5a_O t_v^2 + (t_A - t_v)\Delta v_{OAC}\right] = t_A\Delta v_{OA} \tag{86}$$

Likewise, multiplying (84) by $-\sin\chi_O$, (85) by $\cos\chi_O$, and adding the resulting equations together allows the track angle maneuver component to be isolated:

$$\left[0.5\omega_O t_\chi^2 + (t_A - t_\chi)\Delta\chi_{OAC}\right] = t_A\Delta\chi_{OA} \tag{87}$$

Hence, under the linearity assumptions used, the speed and track angle maneuvers can be uncoupled.

6.3 Speed Avoidance Maneuver

Substituting (75) into (86):

$$\left(\frac{1}{2a_O}\right)(\Delta v_{OAC})^2 - t_A\Delta v_{OAC} + t_A\Delta v_{OA} = 0 \tag{88}$$

The commanded speed maneuver, Δv_{OAC}, that is a solution to the polynomial (88) is [4]:

$$\Delta v_{OAC} = a_O\left\{t_A - \sqrt{t_A^2 - \left(\frac{2t_A\Delta v_{OA}}{a_O}\right)}\right\} \tag{89}$$

This maneuver is subject to the constraint that:

$$|\Delta v_{OA}| \le 0.5t_A|a_O| \tag{90}$$

Equations (89) and (90) are general enough to also apply to the case where:

$$\Delta v_{OA} < 0 \tag{91}$$

In that case, a deceleration is required where:

$$a_O < 0 \tag{92}$$

As will be discussed in a later section, the feasible speed maneuvers may be limited by a minimum and maximum speed limit, $v_{O,MIN}$ and $v_{O,MAX}$:

$$v_{O,MIN} \le (v_O + \Delta v_{OAC}) \le v_{O,MAX} \tag{93}$$

If (93) is not satisfied, the avoidance speed maneuver is not feasible. However, if the avoidance maneuver is an optimum maneuver, using both speed and track angle to avoid the intruder, the commanded speed in (88) can be set to the corresponding limit:

$$v_{OAC} = v_{O,MAX} \tag{94}$$

or,

$$v_{OAC} = v_{O,MIN} \tag{95}$$

Substituting (94) or (95) into (88) leads to the feasible instantaneous speed maneuvers:

$$v_{OA} = v_{O,MAX} - \left[\frac{(v_{O,MAX} - v_O)^2}{2 a_O t_A} \right] \tag{96}$$

or,

$$v_{OA} = v_{O,MIN} + \left[\frac{(v_O - v_{O,MIN})^2}{2 |a_O| t_A} \right] \tag{97}$$

The corresponding avoidance track angle maneuver can then be obtained using (15) as follows:

$$\chi_{OA} = \chi_A - \arcsin\left\{ \left(\frac{v_I}{v_{OA}} \right) \sin(\chi_A - \chi_I) \right\} \tag{98}$$

6.4 Track Angle Avoidance Maneuver

Now to determine the commanded track angle maneuver, substitute (78) into (87):

$$(\Delta\chi_{OAC})^2 - (2 t_A \omega_O) \Delta\chi_{OAC} + (2 t_A \omega_O \Delta\chi_{OA}) = 0 \tag{99}$$

This can be solved as follows [4]:

$$\Delta\chi_{OAC} = \omega_O \left\{ t_A - \sqrt{t_A^2 - \left(\frac{2t_A \Delta\chi_{OA}}{\omega_O} \right)} \right\} \tag{100}$$

This maneuver is subject to the constraint that:

$$\left|\Delta\chi_{OA}\right| \le 0.5 t_A \left|\omega_O\right| \tag{101}$$

Equations (100) and (101) are general enough to also apply to the case where:

$$\Delta\chi_{OA} < 0 \tag{102}$$

In that case a negative turn rate is required:

$$\omega_O < 0 \tag{103}$$

6.5 Recovery Speed Maneuver

Equation (88) can be adapted to describe the commanded recovery maneuver problem:

$$\left(\frac{1}{2a_O} \right) \left(\Delta v_{ORC} \right)^2 - t_R \Delta v_{ORC} + t_R \Delta v_{OR} = 0 \tag{104}$$

In (104), Δv_{ORC}, is the commanded speed change:

$$\Delta v_{ORC} \equiv \left(v_{ORC} - v_{OAC} \right) \tag{105}$$

Also, Δv_{OR}, is the desired (instantaneous) speed change from the last speed:

$$\Delta v_{OR} \equiv \left(v_{OR} - v_{OAC} \right) \tag{106}$$

The solution to (104) is:

$$\Delta v_{ORC} = a_O \left\{ t_R - \sqrt{t_R^2 - \left(\frac{2t_R \Delta v_{OR}}{a_O} \right)} \right\} \tag{107}$$

The commanded recovery speed maneuver in (107) is subject to the constraint that:

$$\left|\Delta v_{OR}\right| \le 0.5 t_R \left|a_O\right| \tag{108}$$

As will be discussed in a later section, the feasible speed maneuvers are limited by a minimum and maximum speed limit, $v_{O,MIN}$ and $v_{O,MAX}$:

$$v_{O,MIN} \le (v_{OAC} + \Delta v_{ORC}) \le v_{O,MAX} \tag{109}$$

If (109) is not satisfied, the recovery speed maneuver is not feasible. However, if the recovery maneuver is used to acquire a moving waypoint, such as a MIT slot, both a recovery speed and track angle maneuver is required. Hence, the commanded speed in (109) can be set to the nearest speed limit:

$$v_{ORC} = (v_{OAC} + \Delta v_{ORC}) = v_{O,MAX} \tag{110}$$

or,

$$v_{ORC} = (v_{OAC} + \Delta v_{ORC}) = v_{O,MIN} \tag{111}$$

Substituting (110) or (111) into (104) leads to the feasible instantaneous speed maneuvers:

$$v_{OR,MAX} = v_{O,MAX} - \left[\frac{(v_{O,MAX} - v_{OAC})^2}{2 a_O t_R} \right] \tag{112}$$

or,

$$v_{OR,MIN} = v_{O,MIN} + \left[\frac{(v_{OAC} - v_{O,MIN})^2}{2 |a_O| t_R} \right] \tag{113}$$

Now for the recovery to a MIT slot, it is desirable to return back to this slot as soon as possible. This is achieved by selecting the arbitrary relative recovery speed, V_R, using (112) in (44):

$$V_R = -v_{WP} \cos(\mathrm{X}_R - \chi_{WP}) + \sqrt{v_{OR,MAX}^2 - v_{WP}^2 \sin^2(\mathrm{X}_R - \chi_{WP})} \tag{114}$$

Using (114) in (40) and (41) yields the recovery maneuver with the shortest feasible recovery time.

$$v_{OR} = \sqrt{V_R^2 + 2 v_{WP} V_R \cos(\mathrm{X}_R - \chi_{WP}) + v_{WP}^2} \tag{115}$$

and

$$\chi_{OR} = \arctan\left[\frac{V_R \sin \mathrm{X}_R + v_{WP} \sin \chi_{WP}}{V_R \cos \mathrm{X}_R + v_{WP} \cos \chi_{WP}} \right] \tag{116}$$

The corresponding commanded recovery speed, Δv_{ORC}, is obtained by substituting (115) into (107).

6.6 Recovery Track Angle Maneuver

In a similar manner, (99) can be adapted to define the commanded recovery track angle maneuver problem:

$$(\Delta\chi_{ORC})^2 - (2t_R\omega_O)\Delta\chi_{ORC} + (2t_R\omega_O\Delta\chi_{OR}) = 0 \tag{117}$$

In (117), $\Delta\chi_{ORC}$, is the commanded speed change:

$$\Delta\chi_{ORC} \equiv (\chi_{ORC} - \chi_{OAC}) \tag{118}$$

Also, $\Delta\chi_{OR}$, is the desired (instantaneous) speed change from the last speed:

$$\Delta\chi_{OR} \equiv (\chi_{OR} - \chi_{OAC}) \tag{119}$$

The solution to (117) is:

$$\Delta\chi_{ORC} = \omega_O\left\{t_R - \sqrt{t_R^2 - \left(\frac{2t_R\Delta\chi_{OR}}{\omega_O}\right)}\right\} \tag{120}$$

The commanded recovery track angle maneuver in (120) is subject to the constraint that:

$$|\Delta\chi_{OR}| \le 0.5t_R|\omega_O| \tag{121}$$

7 Aircraft Speed Maneuver Constraints

In general, the magnitude of the track angle maneuver that an aircraft can perform is not constrained – although large angle maneuvers are undesirable. However, aircraft aerodynamic and propulsive considerations limit the speed maneuvers that can be executed.

A typical jet aircraft maneuver envelope is shown in Figure 12:

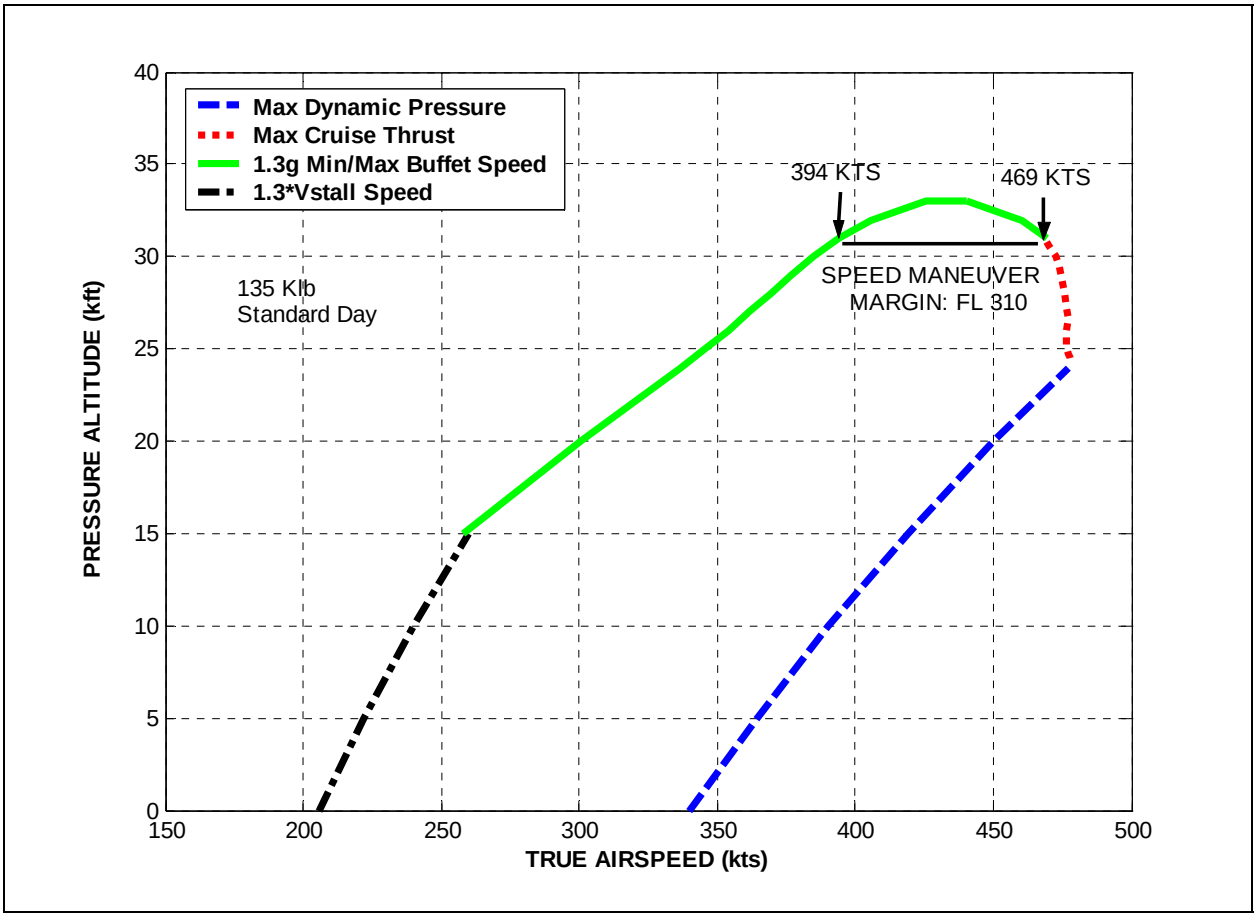

Figure 12. DC-9-80 Series Aircraft Maneuver Envelope

For any given altitude, a jet aircraft is limited to a minimum and maximum cruise speed due to a number of constraints:

- maximum structural loading,
- engine thrust, and
- aerodynamic buffeting.

The four categories of speeds that typically dominate aircraft maneuver limitations are:

- normal operating speed,
- maximum level flight speed,

- minimum / maximum buffet speeds, and
- stall speed.

At the higher end of the speed regime (especially at lower altitudes) is the aircraft's normal operating speed, V_{NO}. The normal operating speed, also known as the maximum structural cruising speed, is the maximum speed that an aircraft should fly under normal operating conditions. For a DC-9-80 (MD-80) aircraft, representative of current technology transport aircraft, the normal operating speed is V_{NO} = 340 kts calibrated airspeed [5].

At the higher end of the speed regime (especially at higher altitudes) is the aircraft's maximum level flight cruise speed. This speed is the maximum straight-and-level speed that an aircraft can fly due to the maximum available thrust of the engines to match the rapidly-rising airframe drag at high speeds. This speed limit is primarily a function of the airframe drag coefficient characteristic and engine lapse rate. In Figure 12, the maximum cruise thrust characteristic for the 135Klb MD-80 was taken from [5].

Next, at the lower end of the speed regime and at the highest altitudes, are the minimum and maximum buffet speeds. These buffet speeds limit how slow or fast an aircraft can fly without experiencing significant airframe vibration. At higher subsonic Mach numbers, the buffet speed can limit the aircraft to minimum speeds significantly higher than the stall speed. The buffet speed or Mach number is given by:

$$V_B = aM_B = \sqrt{\frac{2nW}{S\rho C_{L_{MAX\ buffet}}}} \tag{122}$$

where: V_B = buffet speed
M_B = buffet Mach number
a = speed of sound at given altitude
n = load factor
W = aircraft weight
S = wing (reference) area
ρ = atmospheric density
$C_{L_{MAX\ buffet}}$ = maximum aircraft lift coefficient due to buffet

For a given aircraft, $C_{L_{MAX\ buffet}}$ is typically a nonlinear function of Mach number as illustrated in Figure 13.

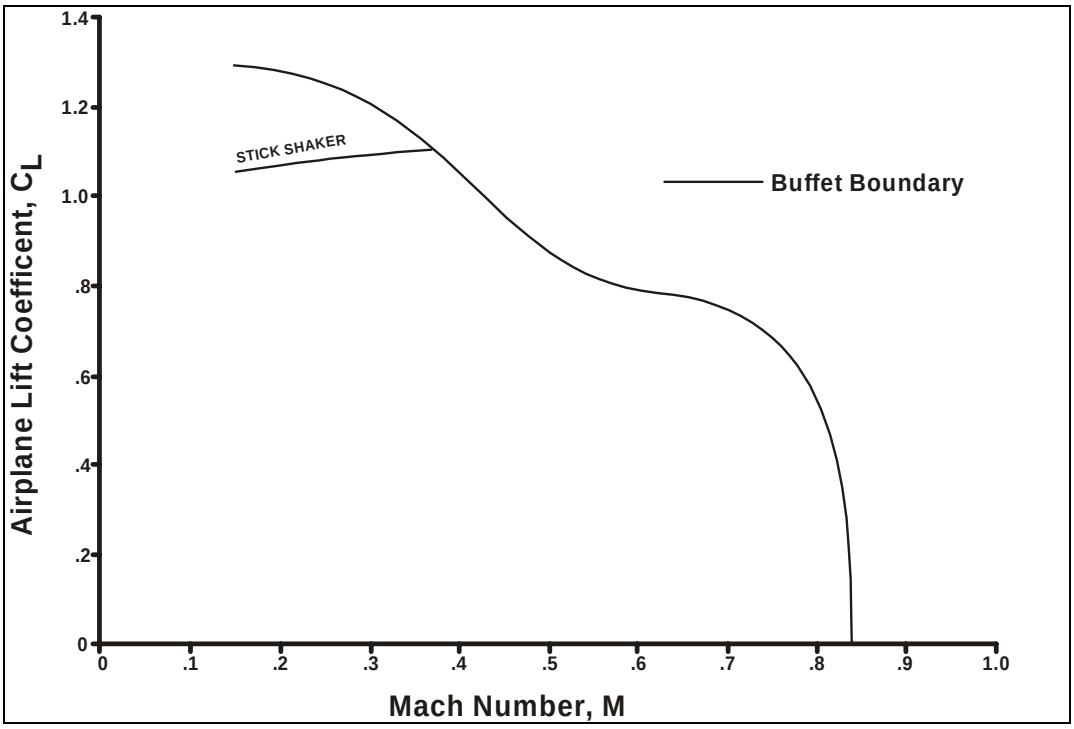

Figure 13. DC-9-80 Series Maximum Buffet Lift Coefficient as a Function of Mach [5]

The reason that both minimum and maximum buffet speeds exist results from the fact that both low-speed and high-speed cruise flight at high altitudes may require aircraft lift coefficients which run up against transonic/Mach-based airframe buffet limitation. The existence of both minimum and maximum buffet speeds due to the same lift coefficient characteristic is analytically shown in the multiple intersections of (122) with the buffet lift coefficient characteristic from Figure 13, as shown in Figure 14.

Operationally, the aircraft buffet speed limits normally include a load factor margin for safely handling of high-altitude turbulence. A typical load factor margin chosen is 0.3 g's. In Figure 12, the minimum and maximum buffet speeds for the 135Klb MD-80 were determined based on flight with a 0.3g load factor margin and the aircraft buffet lift coefficient characteristic taken from [5] and shown in Figure 13.

Finally, at lower Mach numbers, the buffet speeds yield to the stall speed in importance. At lower altitudes and speeds, airflow separation over the aircraft wing airfoils limit the ability for the aircraft to generate sufficient lift to keep the aircraft airborne. This aircraft performance limit is driven by the stall speed of a given aircraft configuration. Stall speed is a function of a number of factors including aircraft weight, wing area, airfoil shape, and configuration (e.g., deployed flaps and slats). The low-speed, low altitude stall limit typically includes a safety margin equal to 0.3 times the stall speed. In Figure 12, the minimum stall speed characteristic for the 135Klb MD-80 was determined based on 1.3 times the designated stall speed of 167 kts calibrated airspeed taken from [5].

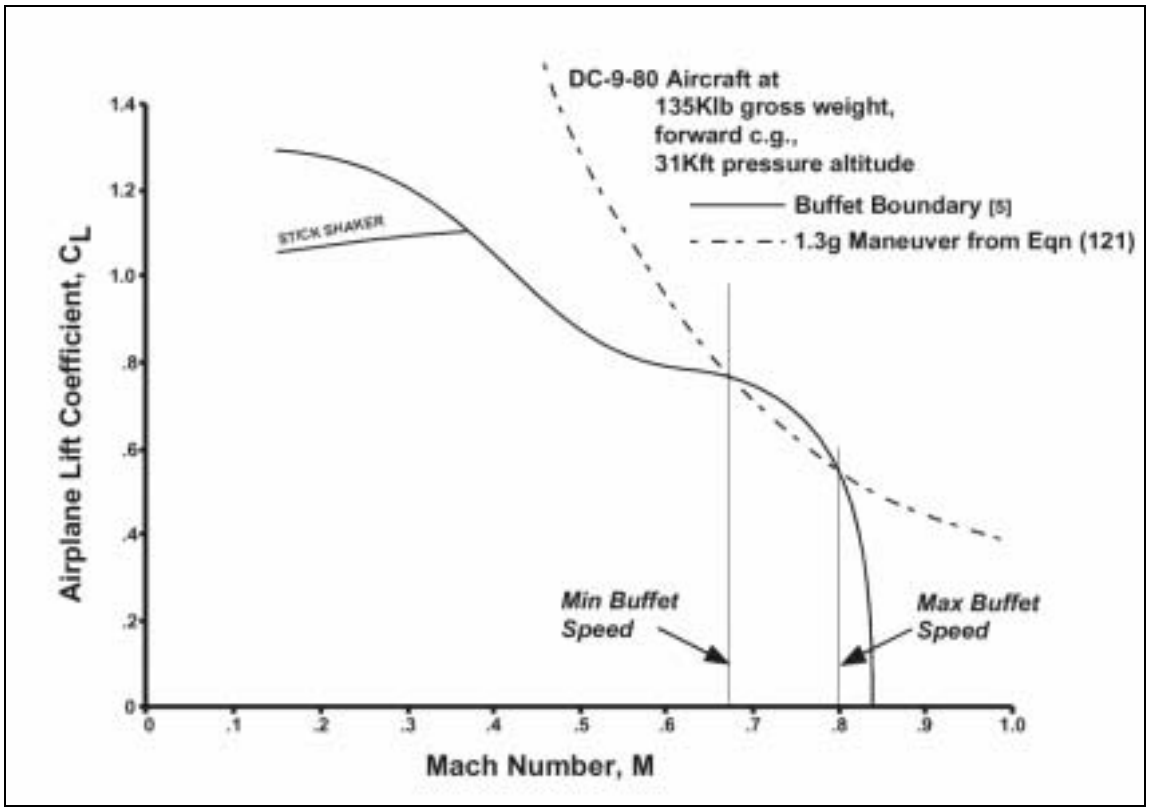

Figure 14. DC-9-80 Series Min and Max Buffet Speed Solutions

Using [5], the above maneuver envelope limits were calculated for a DC-9-80 aircraft in a cruise configuration flying at a weight of 135,000 lb and at standard-day conditions. The resulting maneuver envelope is shown in Figure 12. As one can see, at the lower altitudes, the stall speed and maximum dynamic pressure limitations dominate. At the higher altitudes, the buffet speeds and engine thrust limitations dominate.

For the DC-9-80 performance envelope, the maximum speed maneuver margin (i.e., the difference between maximum aircraft speed and minimum aircraft speed for a given altitude) occurs at 15Kft pressure altitude. At typical cruise altitudes (≥ 29Kft pressure altitude), the speed window shrinks quite rapidly before going to zero. At altitudes lower than 15Kft pressure altitude, this speed maneuver margin gets smaller, but this decrease, as a function of altitude change, is slow and does not go to zero.

In the operational National Air Space (NAS) environment, in addition to aircraft performance limitations, the usable speed maneuver margin will be a function of other real-world limits. These limits include additional conservatism in selecting the maximum and minimum speeds due to flight management system (FMS) limits, ATM automation performance modeling, airline policy, and pilot acceptability. An interesting phenomenon to note is that the shape of the maneuver envelope is such that lines of constant calibrated airspeed (CAS) (e.g., parallel to the “Max Dynamic Pressure” limit)

will tend to either be feasible or infeasible over normal operating ranges of the aircraft and independent of altitude. This behavior of the constant CAS lines leads to the possibility of a quick, CAS-based maneuver heuristic (e.g., “avoid the conflict by slowing to 250 kts CAS”) that could be operationally used by pilots. In discussions with line pilots, the authors have discovered some evidence of this real-world heuristic.

The trends observed in the speed maneuver margin lead to the conclusion that aircraft performance limitations are a significant constraint on feasible conflict avoidance and resolution maneuvers. As is the case for the DC-9-80, we expect the set of feasible maneuvers to decrease as altitude increases for the typical, turbofan-powered commercial aircraft at normal, en route cruising altitudes.

8 Performance Metric

8.1 Definition

The intent of a maneuver performance metric is to determine the merits of alternate maneuvers without using a high-fidelity aircraft simulation. Hence, when properly chosen, the metric adequately captures the quantitative impact of the penalties incurred with alternate maneuvers.

The key performance metric of interest to the airlines is the change in the direct operating cost (*DOC*) when conflict resolution maneuvers are performed. The *DOC* is defined as:

$$DOC = b_t \Delta t + b_F \Delta w_F \tag{123}$$

In (123), b_t and b_F are the time and fuel costs respectively. In addition, Δt and Δw_F are the time interval of interest and the fuel weight expended over this time interval, respectively:

$$\Delta w_F = \int_0^{\Delta t} \dot{w}_F dt \tag{124}$$

In (124), $\dot{w}_F$ is the aircraft fuel consumption rate.

Using (123) and (124) and the cost index, $c_I \equiv \frac{b_T}{b_F}$, the efficiency metric (*EM*) is defined as:

$$EM \equiv \left(\frac{DOC_{NOM}}{DOC_{CD\&R}} \right) = \frac{c_I t_{NOM} + \int_0^{t_{NOM}} \dot{w}_{F,NOM} dt}{c_I (t_A + t_R) + \left(\int_0^{t_A} \dot{w}_{F,A} dt + \int_0^{t_R} \dot{w}_{F,R} dt \right)} \tag{125}$$

8.2 Fuel Weight Expended

Based on [6], the fuel consumption rate at cruise altitude is proportional to the thrust:

$$\dot{w}_F = c_F \left(1 + \frac{v}{c_{F2}} \right) T \tag{126}$$

In (126), T is the aircraft thrust, v is the true airspeed, c_F is the composite specific fuel consumption coefficient, and c_{F2} is cruise fuel flow airspeed correction factor.

Under steady state, non-accelerating, conditions (when any speed change has been completed), the thrust, *T*, must equal the drag, *D*:

$$T \cong D \equiv 0.5\rho v^2 S C_D \tag{127}$$

where, ρ = atmospheric pressure at the cruise altitude
S = aerodynamic reference area
C_D = aerodynamic drag coefficient.

Substituting (127) into (126):

$$\dot{w}_F = 0.5 c_F \rho S \left(1 + \frac{v}{c_{F2}}\right) v^2 C_D(v) \tag{128}$$

Substituting (128) into (124):

$$\Delta w_F = \int_0^{\Delta t} \dot{w}_F dt = 0.5 c_F \rho S \int_0^{\Delta t} \left(1 + \frac{v}{c_{F2}}\right) v^2 C_D(v) dt \tag{129}$$

8.3 Speed Maneuver

The drag coefficient, C_D, in (129) is [6]:

$$C_D \equiv C_{D0} + C_{D2} C_L^2 \tag{130}$$

where C_{D0}, C_{D2} = aerodynamic drag coefficient parameters
C_L = aerodynamic lift coefficient

To determine the lift coefficient, C_L, the equation for lift is used:

$$L \equiv 0.5\rho v^2 S C_L \tag{131}$$

For level flight, lift equals the weight of the aircraft:

$$L = W \tag{132}$$

Hence, combining (131) and (132), the lift coefficient for level flight is:

$$C_L \cong \frac{2W}{\rho v^2 S} \tag{133}$$

Substituting (133) into (130):

$$C_D \equiv C_{D0} + C_{D2} \left(\frac{2W}{\rho v^2 S}\right)^2 \tag{134}$$

8.4 Track Angle Maneuver

The standard track angle maneuver is performed using a coordinated turn. The coordinated turn increases the lift of the aircraft by increasing the angle of attack. With the increased lift, the aircraft is rolled (banked) into the direction of the desired turn. By keeping the size of the lift and roll angle coordinated, the vertical component of the lift remains equal to the weight of the aircraft. The lateral component of the lift, divided by the speed of the aircraft determines the turning rate:

$$\dot{\chi}_{CT} = \frac{L_{CT} \sin\mu}{v}\left(\frac{g}{W}\right) \tag{135}$$

where, $\dot{\chi}_{CT}$ = aircraft track angle rate using a coordinated turn
L_{CT} = lift required for coordinated turn
μ = bank (roll) angle
g = gravitational acceleration

For a coordinated turn: $$L_{CT}\cos\mu = W \tag{136}$$

Combining (135) and (136), track angle rate for a coordinated turn is:

$$\dot{\chi}_{CT} = \frac{g\tan\mu}{v} \tag{137}$$

For a coordinated turn, the lift coefficient is obtained by combining (129) and (136):

$$C_{L,CT} \cong \frac{2W}{\rho v^2 S\cos\mu} \tag{138}$$

Substituting (138) into (130):

$$C_D \equiv C_{D0} + C_{D2}\left(\frac{2W}{\rho v^2 S\cos\mu}\right)^2 \tag{138}$$

The drag coefficient of the MD-80 aircraft at a cruise altitude of 31,000 ft is illustrated in Figure 15, based on [5]. It is also described more completely in Appendix A. This figure shows how the drag coefficient varies with the true airspeed under normal level flight conditions as well as for a nominal and a maximum coordinated turn. The aircraft uses either of the coordinated turn drag coefficient curves only during the time that a non-zero turn rate is required to achieve a new track angle.

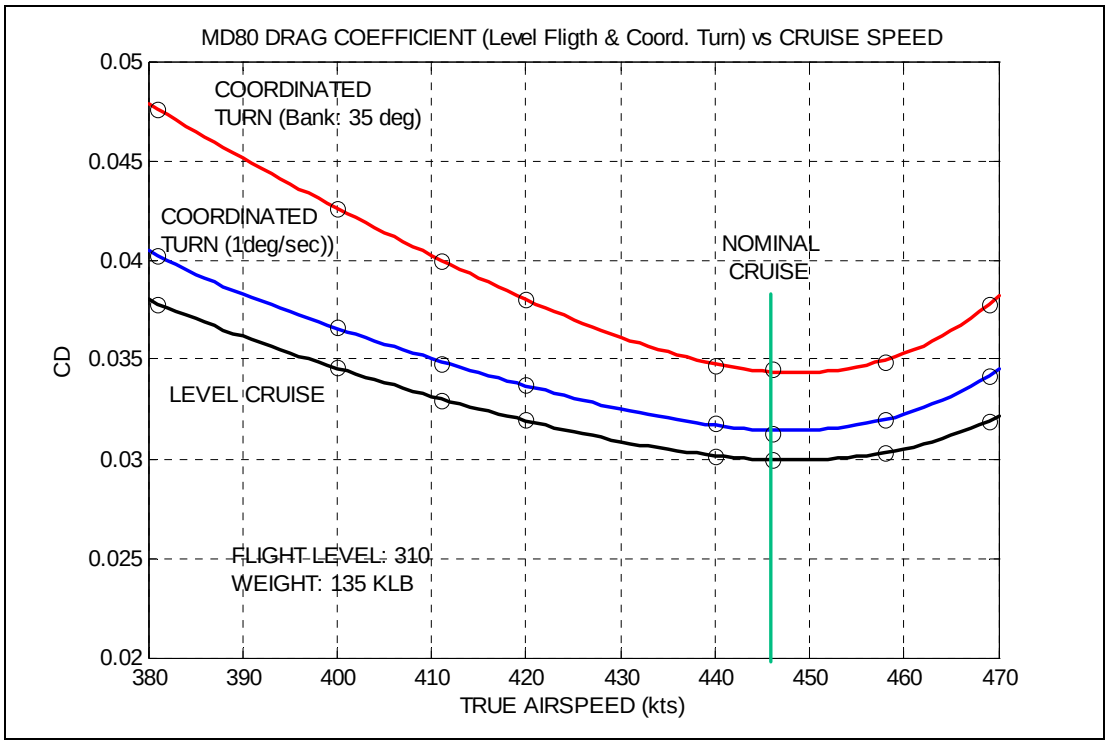

Figure 15. MD-80 Cruise Drag Coefficient vs True Airspeed
(FL 310, Weight 135Klb)

8.5 Efficiency Metric

If the speed, *v*, is constant over the time interval of integration, Δt, then (129) simplifies to:

$$\Delta w_F = \int_0^{\Delta t} \dot{w}_F dt = 0.5 c_F \rho S \left(1 + \frac{v}{c_{F2}}\right) v^2 C_D(v) \Delta t \tag{139}$$

If the aircraft is changing speed without changing the track angle, then the drag coefficient, $C_D(v)$, defined by (134). Alternately, if the aircraft is changing its track angle, with or without changing its speed, then the drag coefficient defined by (138) is used.

Hence, for instantaneous avoidance and recovery speed and/or track angle maneuvers, substituting (139) into (125) leads to:

$$EM = \frac{b_t t_{ETA} + 0.5 b_F c_F \rho S \left(1 + \frac{v_O}{c_{F2}}\right) v_O^2 C_D(v_O) t_{ETA}}{b_t (t_A + t_R) + 0.5 b_F c_F \rho S \left[\left(1 + \frac{v_{OA}}{c_{F2}}\right) v_{OA}^2 C_D(v_{OA}) t_A + \left(1 + \frac{v_{OR}}{c_{F2}}\right) v_{OR}^2 C_D(v_{OR}) t_R\right]} \tag{140}$$

When acceleration or turn rate maneuvers are performed, the efficiency metric has to solve (125). This is accomplished using numerical integration of the respective fuel weight flow integrals.

The direct operating cost rate for level flight without turns is illustrated in Figure 16 for the MD-80 aircraft at a cruise altitude of 31,000 ft with a weight of 135,000 lb. Also shown are the speed maneuver limits for this aircraft as derived in the previous section, while the nominal cruise speed for this aircraft at this altitude is Mach 0.76 or 446 kts. The curve in Figure 16 can be used together with the maneuver times and speeds required in (140) to evaluate this efficiency metric. The units used in Figure 16 and (140) must, however, be consistent.

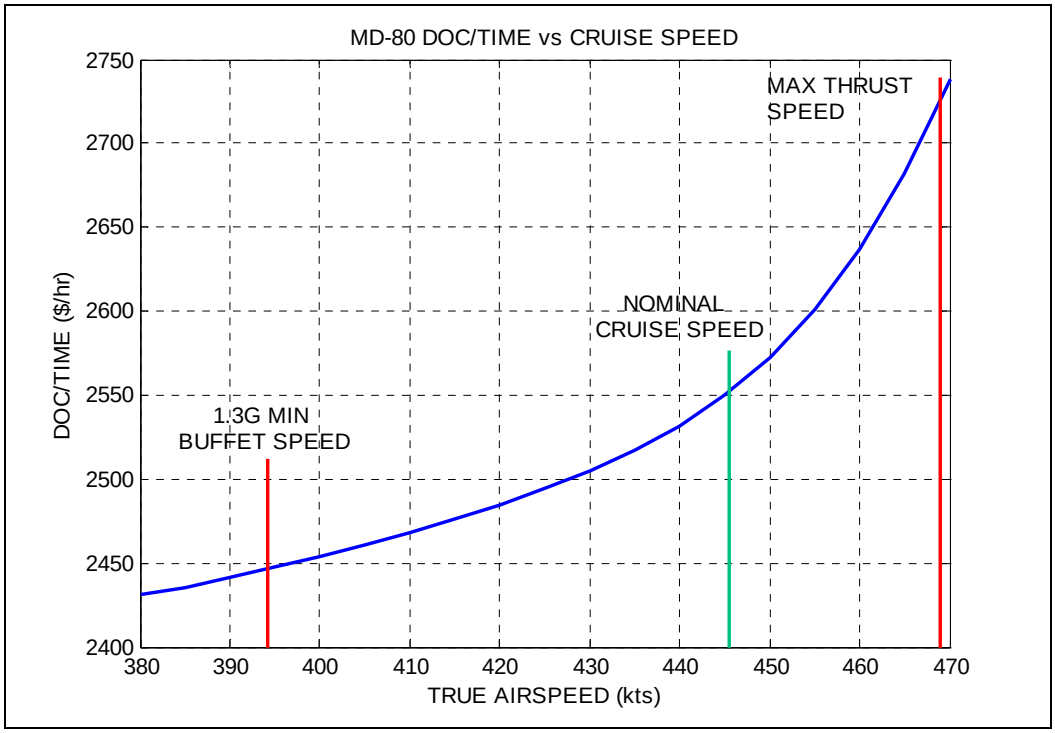

Figure 16. MD-80 Total Direct Operating Cost Rate vs True Airspeed
(FL 310, Weight: 135 Klb)

9 Fixed Crossing Angle Test Cases

9.1 Test Case Description

A number of CD&R cases are investigated to illustrate the avoidance and recovery maneuvers as well as their performance. The initial conditions for the test cases are summarized in Table 1. In Table 1, the MIT conditions correspond to the special case where the own aircraft is forced out of a MIT stream of traffic due to a potential conflict with an intruder aircraft. After the avoidance maneuver, the own aircraft returns back to its original slot.

Table 1. Initial Conditions for Test Cases

	North Position (nm)	**East Position** (nm)	**Speed** (kts)	**Track Angle** (deg)
Own Aircraft	**40**	**0**	**446**	**180**
Intruder Aircraft	**0**	**-40**	**446**	**90**
Hazard (Stationary)	**(0,-10), (10,-5), (5,5), (-5,10), (-10,0)**		**0**	**0**
Hazard (Moving)	**(0,-10), (10,-5), (5,5), (-5,10), (-10,0)**		**20**	**90**
Waypoint (Stationary)	**-60**	**0**	**0**	**0**
Waypoint (MIT)	**40**	**0**	**446**	**180**

The hazard region is a pentagon-sized area that is on the flight path of the own aircraft. In the case where the hazard region moves, it is already blocking the normal flight of the own aircraft to its next waypoint at the time of conflict detection. Since it moves so slowly, it remains in front of the own aircraft until an avoidance maneuver is used.

To evaluate the efficiency metric, typical aircraft parameter values for a range of aircraft, are presented in Table 2, based primarily on [6]. In addition the time cost parameters are based on [7] and the fuel cost parameters are based on [8].

Using the parameter values of Table 2 for the MD-80 and the speed constraints of Section 7, minimum and maximum speeds at a cruise altitude of 31,000 feet (FL 310) were computed for a MD-80. The minimum and maximum speeds at this altitude are respectively 394 and 469 knots. Hence, if the MD-80 has a nominal cruise speed of 446 kts (Mach 0.76), then the available speed maneuver limits are: -52 kts and +23 kts. Figure 15 presents the cruise drag coefficient for the MD-80 both for nominal level flight as well as for a nominal and a maximum coordinated turn maneuver. Further discussions about the aerodynamic performance of the MD-80 can be found in Appendix A.

Table 2. Aircraft Performance Parameters [6]

Symbol	Description	Cruise Values					
		MD-80	**B-737**	**B-727**	**B-757**	**B-767**	**B-777**
	Aircraft FAA Type (nJ - n jet engines, L – large jet, H – heavy jet)	2J/L	2J/L	3J/L	2J/LH	2J/H	2J/H
c_l	Cost index (100 lb/hr, '01)*	144	137	179	190	229	246
b_t	Operating cost ('01 $/hr) [7]++	$1,725	$1,646	$2,144	$2,285	$2,753	$2,955
b_F	Fuel cost ('01 $/lb)+ ['01 $/gallon] [8]	$0.12/lb+, [$0.76/gallon]					
c_F	Composite cruise specific fuel consumption coefficient (1/hr)	0.36	0.51	0.28	0.50	0.46	0.58
c_{F2}	Cruise specific fuel consumption coefficient (kts)	426	1000	250	1450	1430	100,000
S	Aerodynamic reference area (ft^2)	1270	1345	1700	1991	3049	4605
W	Nominal weight (klb)	135	137	163	209	331	465
v_O	Aircraft cruise Mach number (TAS (kts) @ FL 310)	0.76 (446)	0.79 (464)	0.82 (481)	0.78 (458)	0.80 (469)	0.84 (493)
ρ	Air density @ FL 310 (slugs/ft^3) [9]	0.857E-3					

+ Based on jet fuel conversion factor of 6.6 lb/gallon

++Based on 1998 cost data (DOT Form 41) [7] and extrapolated to 2001, assuming a 3 year inflation rate of 10%.

* For use in cost metric algorithm, the cost index has to be expressed in terms of lb/sec

9.2 Intruder Avoidance with Recovery to Fixed Waypoint

Table 3 presents a set of test cases for avoidance of a conflict with an intruder aircraft followed by a recovery to the next waypoint. This table examines both the instantaneous maneuvers and the acceleration or turn rate-limited maneuvers. Also, the recovery maneuvers are investigated with and without an RTA constraint. Finally, the conflict scenarios lead to a perfect collision, if not avoided.

Avoidance maneuvers to the right and to the left are investigated. For this -90 deg crossing angle (intruder minus own aircraft track angle) scenario, a right avoidance maneuver allows the own aircraft to pass behind the intruder. Alternately, a left turn avoidance maneuver results in the own aircraft passing ahead of the intruder. All

maneuvers are referenced to the nominal speed and track angle that the own aircraft had at the time that the conflict was detected.

Table 3. Comparison of Acceleration/Turn Rate-limited with Instantaneous Avoidance and Recovery Maneuvers for Fixed Waypoint (With /Without RTA Constraint)

Avoidance Maneuver Cases	RTA	Accel/Turn Rate Limited Maneuver	Relative Avoidance Maneuvers			Relative Recovery Maneuvers	
			Pass	Speed (kts)	Angle (deg)	Speed (kts)	Angle (deg)
3a) Speed-only	No	No	Behind	-72.7	0	0	0
		Yes		Avoidance Speed Exceeds Limit			
	Yes	No		-72.7	0	+56.2	0
		Yes		Avoidance & Recovery Speed Exceed Limits			
3b) Angle-only	No	No	Behind	0	+10.1	0	-5.9
		Yes		0	+10.2	0	-6.0
	Yes	No		0	+10.1	+6.5	-5.9
		Yes		0	+10.2	+6.7	-6.0
3c) Optimum	No	No	Behind	-41.2	+5.1	0	-2.9
		Yes		-43.6	+5.1	+19.2	-2.9
	Yes	No		-41.2	+5.1	+29.4	-2.9
		Yes		Recovery Speed Exceeds Limit			
3d) Speed-only	No	No	Ahead	+86.8	0	0	0
		Yes		Avoidance Speed Exceeds Limit			
	Yes	No		+86.8	0	-49.8	0
		Yes		Avoidance Speed Exceeds Limit			
3e) Angle-only	No	No	Ahead	0	-10.1	0	+7.8
		Yes		0	-10.2	0	+8.1
	Yes	No		0	-10.1	+9.8	+7.8
		Yes		0	-10.2	+10.4	+8.1
3f) Optimum	No	No	Ahead	+19.1	-7.4	0	+5.7
		Yes		+23.0	-7.4	-0.5	+5.8
	Yes	No		+19.1	-7.4	-8.9	+5.7
		Yes		+23.0	-7.4	-9.8	+5.8

The acceleration-constrained speed maneuvers were computed with a maximum acceleration of +0.2 kts/sec or with a maximum deceleration of -1.2 kts/sec. The turn rate-constrained maneuvers were computed with a turn rate limit of ±1.7 deg/sec. Calculated based on typical high altitude acceleration and idle thrust deceleration rates, for the MD-80 [5] and a turn rate limit based on a 35 deg bank angle limit [6], these limits are applicable to a given MD80 at FL310 with a weight of 135Klb. More extreme deceleration and turn rate maneuvers are physically possible for the MD-80, but in a

real-world operational environment, passenger comfort often plays a factor. Actual deceleration and maximum turn rates are often a function of pilot preference (as discovered by the authors in communications with a number of pilots [10]). In the case of deceleration/accelerations, other factors like pilot perceptions of passenger tolerance of aircraft type-specific acoustic noise and jerk (the change in acceleration) impact pilot control actions. Due to the short time to loss of separation (4.7 min) for this scenario, these acceleration and turn rates are considered to be realistic for a tactical CD&R scenario.

Examining Table 3, the speed avoidance maneuvers are infeasible since the speed limits are exceeded. For the optimum avoidance maneuvers, that use a combination of speed and track angle maneuvers, the instantaneous speed maneuvers were selected such that the acceleration-constrained speed avoidance maneuver does not exceed the speed limit. This can be seen in Case 3f. Since there is no comparable means to recompute the recovery speed maneuvers for the optimum avoidance cases, the RTA-constrained optimum recovery maneuver in Case 3c was found to be infeasible.

In general the difference between the RTA-constrained and unconstrained instantaneous maneuvers is that the former require a recovery speed maneuver while the latter return the recovery speed back to the nominal speed. Also, it is seen that the difference between the acceleration and turn rate constrained maneuvers and the instantaneous maneuvers is small, with the exception of speed maneuvers that require an acceleration, such as Case 3c and 3f.

Figure 17 compares the acceleration/turn rate-constrained maneuvers with the instantaneous maneuvers for the RTA-constrained maneuver of 3c. Similarly, Figure 18 illustrates the RTA-constrained maneuvers of Case 3f.

Table 4 summarizes the acceleration/turn rate constrained track angle and optimum avoidance cases of Table 3. The principal benefit of the RTA-constrained cases is that the time costs are the same for the nominal and the CD&R maneuver case. All the costs that are presented in this table are referenced to the nominal flight costs from the point of conflict detection to the next waypoint.

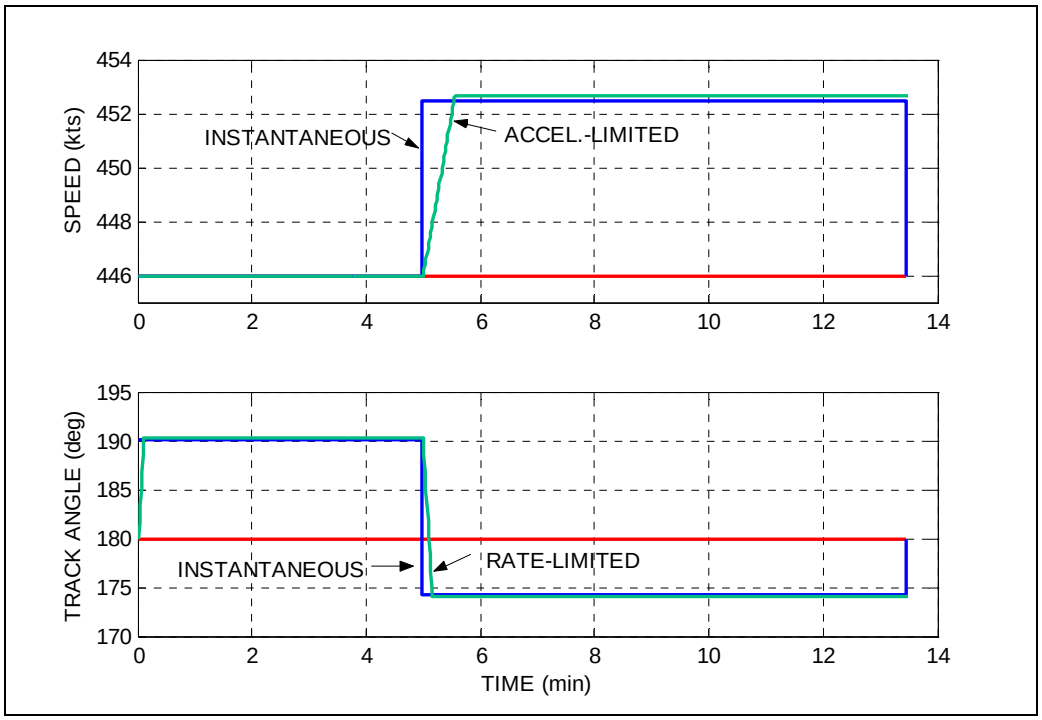

Figure 17. Acceleration/Turn Rate-limited CD&R Maneuvers
(Track Angle-only Avoidance, Pass Behind, RTA)

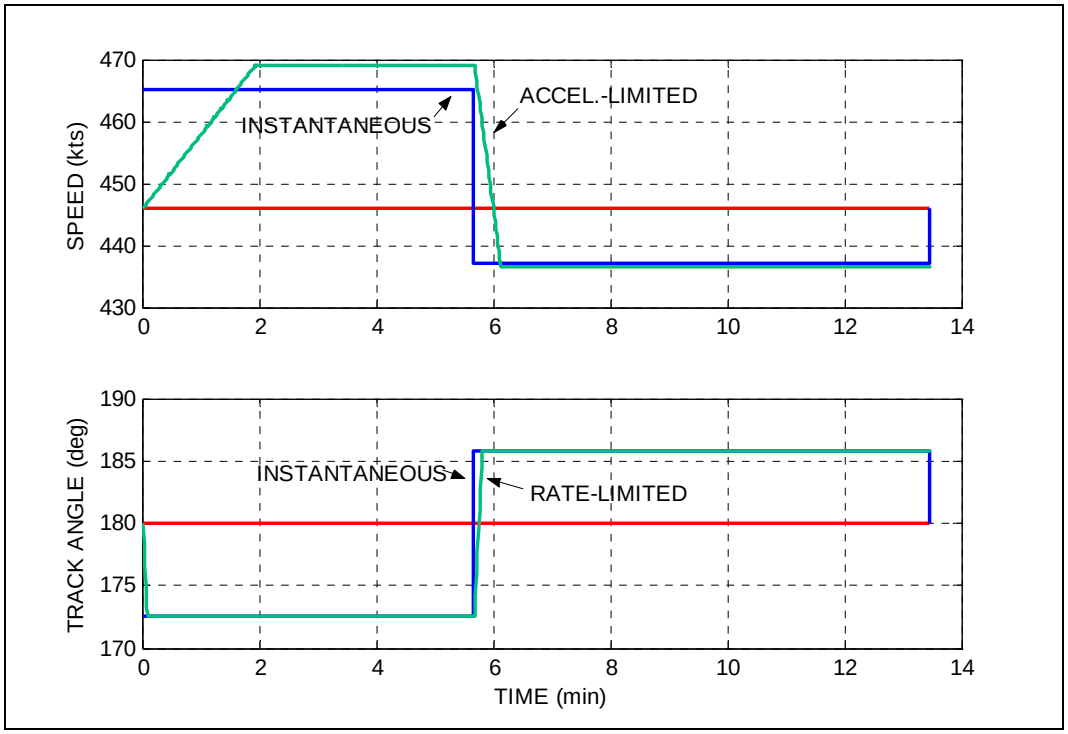

Figure 18. Acceleration/Turn Rate-limited CD&R Maneuvers
(Optimum Avoidance, Pass Ahead, RTA)

Table 4. Avoidance and Recovery Maneuvers for Fixed Waypoint
(With /Without RTA Constraint; Acceleration/Turn Rate-limited Maneuvers)

Avoidance Maneuver Cases	RTA	Relative Avoidance Maneuver			Rel. Recovery Maneuver		Performance Metrics			
		Pass	Speed (kts)	Angle (deg)	Speed (kts)	Angle (deg)	ΔDOC_T ($)	ΔDOC_F ($)	ΔDOC ($)	EM
4a) Angle-only	No	Behind	0	+10.2	0	-6.0	$3.54	$2.53	$6.07	0.990
	Yes		0	+10.2	+6.7	-6.0	0	$5.20	$5.20	0.991
4b) Optimum	No	Behind	-43.6	+5.1	+19.2	-2.9	$15.27	$4.71	$19.98	0.966
	Yes		Recovery Speed Exceeds Limit							
4c) Angle-only	No	Ahead	0	-10.2	0	+8.1	$4.75	$3.02	$7.77	0.987
	Yes		0	-10.2	+10.4	+8.1	0	$7.34	$7.34	0.987
4d) Optimum	No	Ahead	+23.0	-7.4	-0.5	+5.8	-$4.46	$11.73	$7.27	0.988
	Yes		+23.0	-7.4	-9.8	+5.8	0	$9.87	$9.87	0.983

Based on the efficiency metric, the track-angle only, pass behind, avoidance maneuvers of Case 4a achieved the highest performance and hence the minimum maneuver direct operating cost. These cases are shown in green in Table 4. In general, the optimum avoidance maneuvers do not achieve as high a performance when compared to the corresponding track angle avoidance maneuver since the former involve speed maneuvers. The speed maneuvers lead to higher fuel costs since these maneuvers must be maintained for the duration of the avoidance or recovery phase. Track angle maneuvers, on the other hand, only generate higher fuel costs during the brief period that a non-zero turn rate is required.

9.3 Hazard Avoidance with Recovery to Fixed Waypoint

Table 5 presents the CD&R maneuvers between an aircraft and a stationary or moving hazard. Both the acceleration/turn rate-constrained maneuvers and the unconstrained (instantaneous) maneuvers are presented. All the maneuvers are RTA-constrained. The first two cases correspond to the CD&R maneuvers to avoid a stationary hazardous region. Since the area hazard is stationary directly in front of the own aircraft, only a track angle-only maneuver is required either to the left or right around the hazard.

The remaining cases correspond to a slowly moving hazard that is directly in front of the own aircraft at detection. Hence, only track angle or optimum maneuvers are feasible. Of the available moving hazard avoidance cases, only the track-angle avoidance maneuver case that leads to a pass behind maneuver is feasible. The remaining cases require recovery speeds that cannot be achieved with the available acceleration levels. Case 5c is illustrated in Figure 19.

Table 5. Comparison of Acceleration/Turn Rate-limited with Instantaneous Avoidance of Hazard and Recovery to Fixed Waypoint (With RTA Constraint)

Avoidance Maneuver Cases	Hazard Motion	Accel/Turn Rate Limited Maneuver	Relative Avoidance Maneuvers			Relative Recovery Maneuvers	
			Pass	Speed (kts)	Angle (deg)	Speed (kts)	Angle (deg)
5a) Angle-only	No	No	Right	0	+14.0	+15.7	-9.5
		Yes		0	+14.2	+17.3	-9.7
5b) Angle-only	No	No	Left	0	-12.5	+16.5	+10.3
		Yes		0	-12.6	+18.5	+10.7
5c) Angle-only	Yes	No	Behind	0	+11.5	+10.2	-7.6
		Yes		0	+11.7	+10.8	-7.9
5d) Optimum	Yes	No	Behind	-12.9	+11.5	+19.5	-7.6
		Yes		Recovery Speed Exceeds Limit			
5e) Angle-only	Yes	No	Ahead	0	-15.0	+25.2	+12.7
		Yes		Recovery Speed Exceeds Limit			
5f) Optimum	Yes	No	Ahead	-10.2	-15.1	+35.5	+12.7
		Yes		Recovery Speed Exceeds Limit			

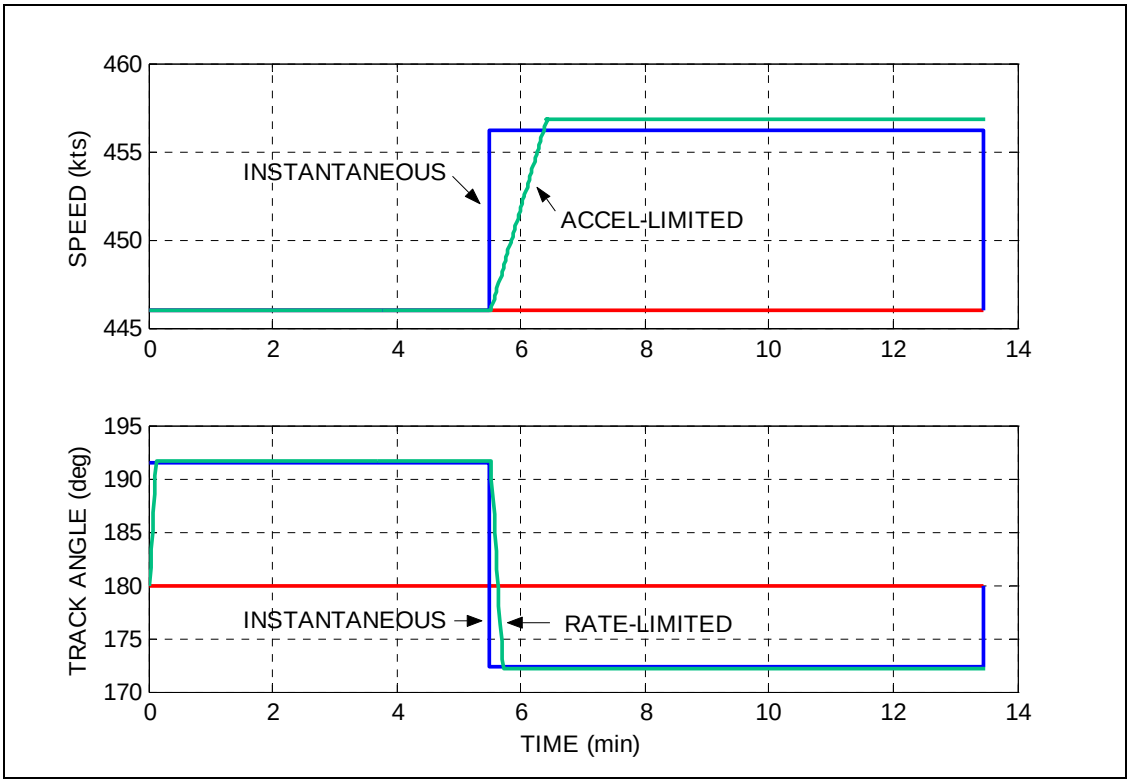

Figure 19. Acceleration/Turn Rate Limited CD&R Maneuvers around Moving Hazard (Heading-only, Pass Behind, RTA-Constraint)

Table 6 presents the performance for the acceleration/turn rate limited cases of Table 5. Of interest is the fact that Cases 6a and 6b have the same efficiency metric to within 3 significant digits, even though there are differences in the magnitudes of the avoidance and recovery maneuvers.

Table 6. Own Aircraft Avoidance of Hazard with Recovery Maneuvers to Fixed Waypoint (Acceleration/Turn Rate-limited Maneuvers, RTA Constraint)

Avoidance Maneuver Cases	*Hazard Motion*	*Relative Avoidance Maneuver*			*Relative Recovery Maneuver*		*Performance Metrics*			
		Pass	**Speed** (kts)	**Angle** (deg)	**Speed** (kts)	**Angle** (deg)	ΔDOC_T ($)	ΔDOC_F ($)	ΔDOC ($)	*EM*
6a) Angle-only	No	Right	0	+14.2	+17.3	-9.9	0	$14.13	$14.13	0.976
6b) Angle-only	No	Left	0	-12.6	+18.5	+10.7	0	$13.99	$13.99	0.976
6c) Angle-only	Yes	Behind	0	+11.7	+10.8	-7.9	0	$7.44	$7.44	0.987
6d) Optimum	Yes	Behind	Recovery Speed Maneuver Exceeds Limit							
6e) Angle-only	Yes	Ahead	Recovery Speed Maneuver Exceeds Limit							
6f) Optimum	Yes	Ahead	Recovery Speed Maneuver Exceeds Limit							

9.4 Intruder Avoidance with Recovery to Moving Waypoint (MIT Constraint)

Table 7 presents four test cases that have the same conflict and avoidance geometry as the previous two-aircraft CD&R scenarios. Now, however the recovery maneuver is back to a moving waypoint and a recovery speed maneuver is always required. However, a recovery track angle maneuver is only required if an avoidance track angle maneuver is used. This table shows both the acceleration/turn rate constrained maneuvers as well as the instantaneous maneuvers.

Table 7. Comparison of Acceleration/Turn Rate-limited with Instantaneous Avoidance and Recovery Maneuvers for Moving Waypoint (Miles-in-Trail Constraint)

Avoidance Maneuver Cases	**Accel/Turn Rate Limited Maneuver**	**Relative Avoidance Maneuvers**			**Relative Recovery Maneuvers**	
		Pass	**Speed (kts)**	**Angle (deg)**	**Speed (kts)**	**Angle (deg)**
7a) Angle-only	No	Behind	0	+10.1	+16.9	-13.4
	Yes		0	+10.2	+23.0	-14.2
7b) Optimum	No	Behind	-41.2	+5.1	+11.5	-1.5
	Yes		-43.6	+5.1	+23.0	-1.5
7c) Angle-only	No	Ahead	0	-10.1	+17.9	+13.4
	Yes		0	-10.2	+23.0	+14.1
7d) Optimum	No	Ahead	+19.2	-7.4	+23.0	+37.2
	Yes		+23.0	-7.4	+23.0	+51.0

While a speed-only avoidance maneuver can be performed for this scenario, it is considered to be infeasible under the MIT constraint. This is based on the fact that this maneuver might violate the miles-in-trail constraint (e.g.: maintain 10 miles in trail ahead and behind the neighboring aircraft in traffic stream).

The recovery maneuvers that are shown in Table 7 are not unique. Specifically, in computing these recovery maneuvers, an unspecified relative recovery speed is required. For the cases in Table 7, the recovery speed was selected such that the fastest feasible recovery would be achieved. This can be seen by examining the acceleration limited recovery speeds for all four cases and noting that these have been set at the maximum positive speed change of +23 kts.

Figure 20 illustrates Case 7a. Case 7d is illustrated in Figures 21 and 22.

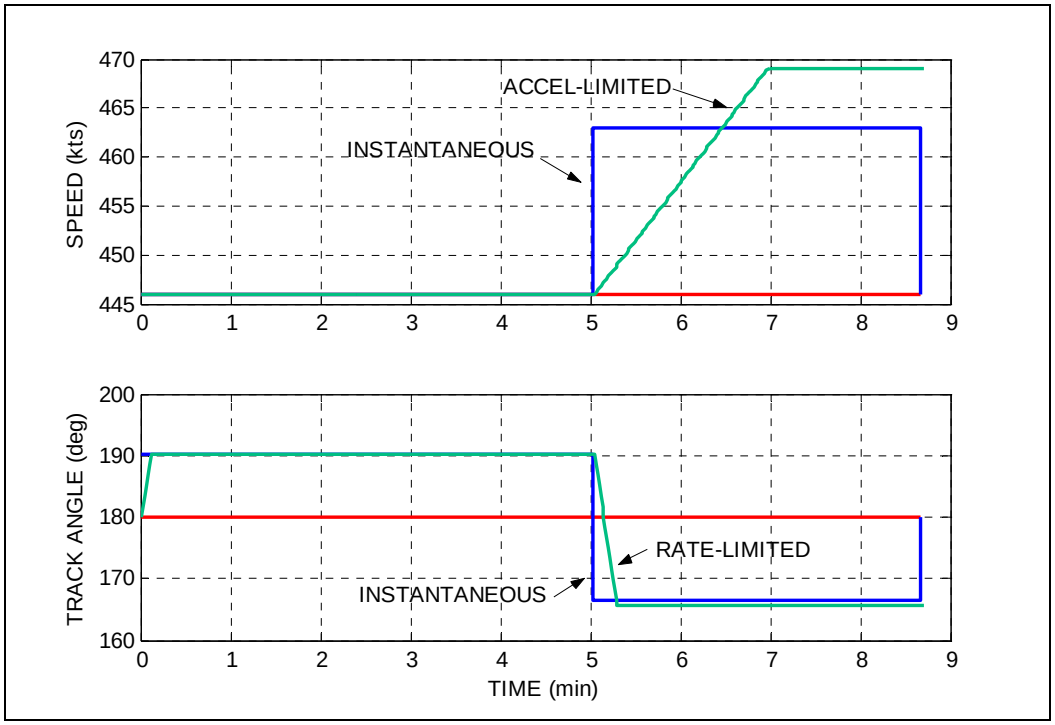

Figure 20. Acceleration/Turn Rate-limited CD&R Maneuvers
(Track Angle-only Avoidance Maneuver, Pass Behind, MIT Constraint)

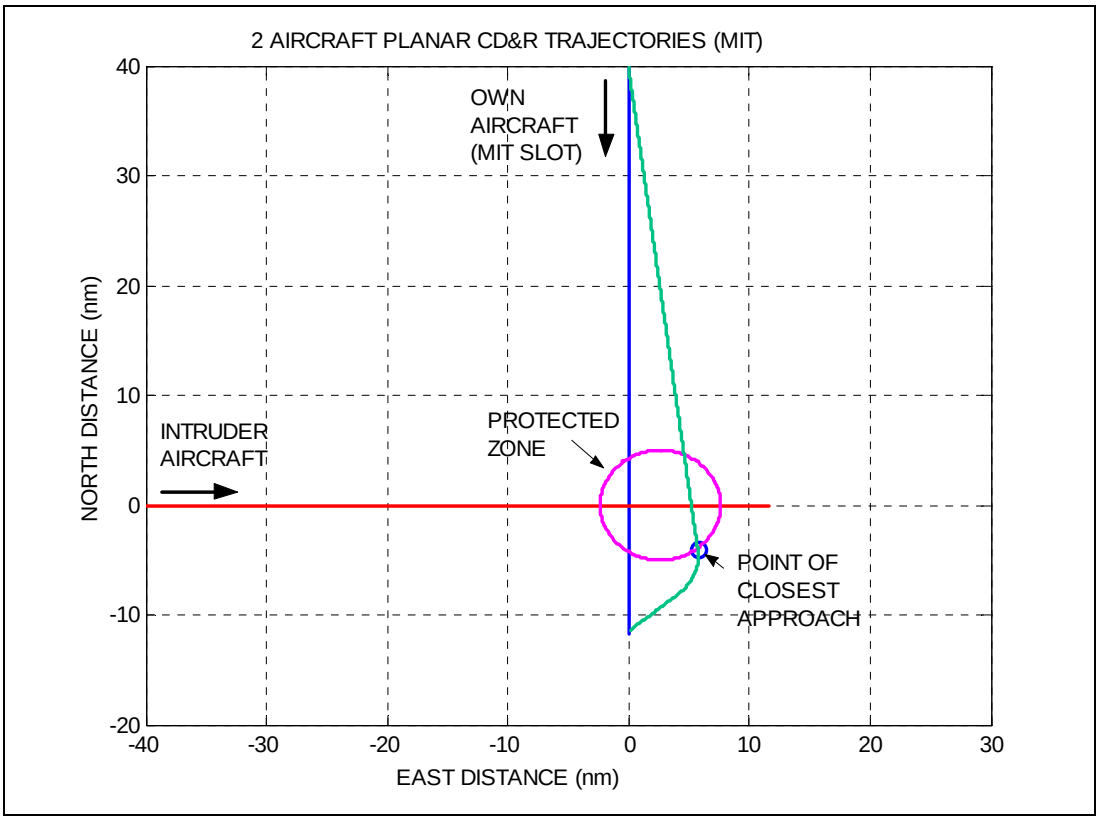

Figure 21. Two Aircraft CD&R Maneuvers (Local Level Coordinates, Optimum Avoidance Maneuver, Pass Ahead, MIT Constraint)

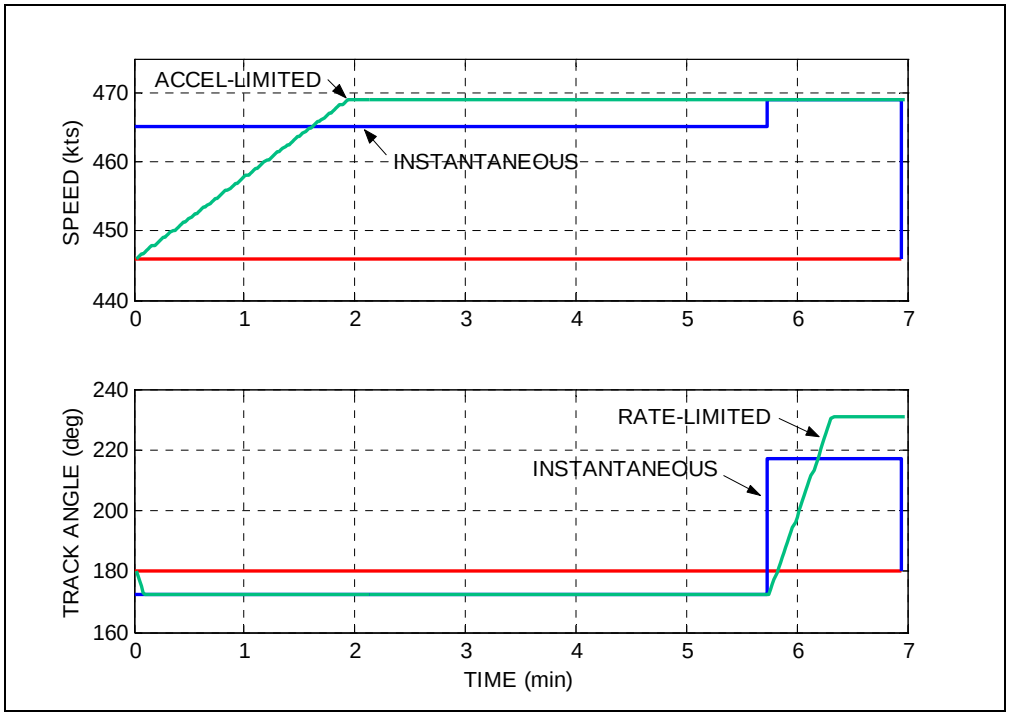

Figure 22. Acceleration/Turn Rate-Limited Aircraft CD&R Maneuvers (Optimum Avoidance Maneuver, Pass Ahead, MIT Constraint)

Finally, Table 8 presents the performance for the acceleration/turn rate limited avoidance and recovery maneuvers in Table 7. The large fuel cost, and low efficiency metric, associated with Case 8b arises from the fact that the actual recovery speed maneuver requires the speed to be changed from -43.6 kts to +23 kts using a maximum acceleration of +0.2 kts/sec. As shown in this table, the track angle avoidance maneuver that leads to a pass behind maneuver, provides the best performance.

Table 8. Avoidance and Recovery Maneuvers to a Moving Waypoint

(Acceleration/Rate-limited Maneuvers, Miles-in-Trail Constraint)

Avoidance Maneuver Cases	*Relative Avoidance Maneuver**			*Relative Recovery Maneuver**		*Performance Metrics*			
	Pass	**Speed** (kts)	**Angle** (deg)	**Speed** (kts)	**Angle** (deg)	ΔDOC_T ($)	ΔDOC_F ($)	ΔDOC ($)	*EM*
8a) Angle-only	Behind	0	+10.2	+23.0	-14.2	0	$8.12	$8.12	0.978
8b) Optimum	Behind	-43.6	+5.1	+23.0	-1.5	0	$21.13	$21.13	0.977
8c) Angle-only	Ahead	0	-10.2	+23.0	+14.1	0	$10.30	$10.30	0.977
8d) Optimum	Ahead	+23.0	-7.4	+23.0	+51.0	0	$18.96	$18.96	0.940

10 Crossing Angle Parametric Test Cases

10.1 Test Case Description

The last section focused on a specific crossing angle conflict scenario, using a -90 degree-crossing angle of the intruder relative to the own aircraft. This section explores the impact of various crossing angles on the conflict evasion performance. The focus is on the two-aircraft conflict case with the own aircraft returning to the next waypoint with a RTA constraint. In addition, the two-aircraft conflict case with a MIT constraint is investigated. The avoidance and recovery maneuvers are assumed to be achieved instantaneously. As shown in the discussion in the last section, the difference between the instantaneous and acceleration/rate-limited maneuvers was only significant for some of the MIT cases.

In the cases presented in this section, the following constraints are invoked:

1. Only the own aircraft maneuvers
2. Own aircraft avoidance maneuver must be completed before next waypoint is reached.
3. Track angle maneuvers (avoidance-nominal or recovery-avoidance) must not exceed 60 degrees.
4. Recovery maneuver must be conflict-free.
5. Speed maneuvers (avoidance-nominal or recovery-nominal) cannot exceed the lower 1.3g buffet limit or the upper max thrust limit.

Constraints 2 and 3 are soft limits that avoid major disruptions of the flight plan. Constraints 4 and 5 represent hard limits that the own aircraft cannot violate.

In the following cases, the crossing angle of the intruder relative to the own aircraft was varied by ten degrees from +10 degrees through 180 degrees to –10 (350) degrees. Since both aircraft start out the same distance from the potential collision point and both have the same initial speed, a zero degree-crossing angle is unrealistic. Two avoidance maneuvers are evaluated: one passing ahead on the front side and one passing behind on the back side of the intruder aircraft.

10.2 Intruder Avoidance with Recovery to Fixed Waypoint (RTA Constraint)

Figures 23 - 25 show the results of the track angle avoidance maneuver cases. Each figure shows both the feasible pass ahead (red) and pass behind (blue) maneuvers. The maneuvers are presented in terms of the change in track angle or speed relative to the nominal case. In Figure 23, the avoidance and recovery speed limits are indicated by the black bands. The avoidance track angle limits are also shown in the top panel.

However, since the recovery track angle limits are measured relative to the avoidance track angle, these limits could not be included in the third panel.

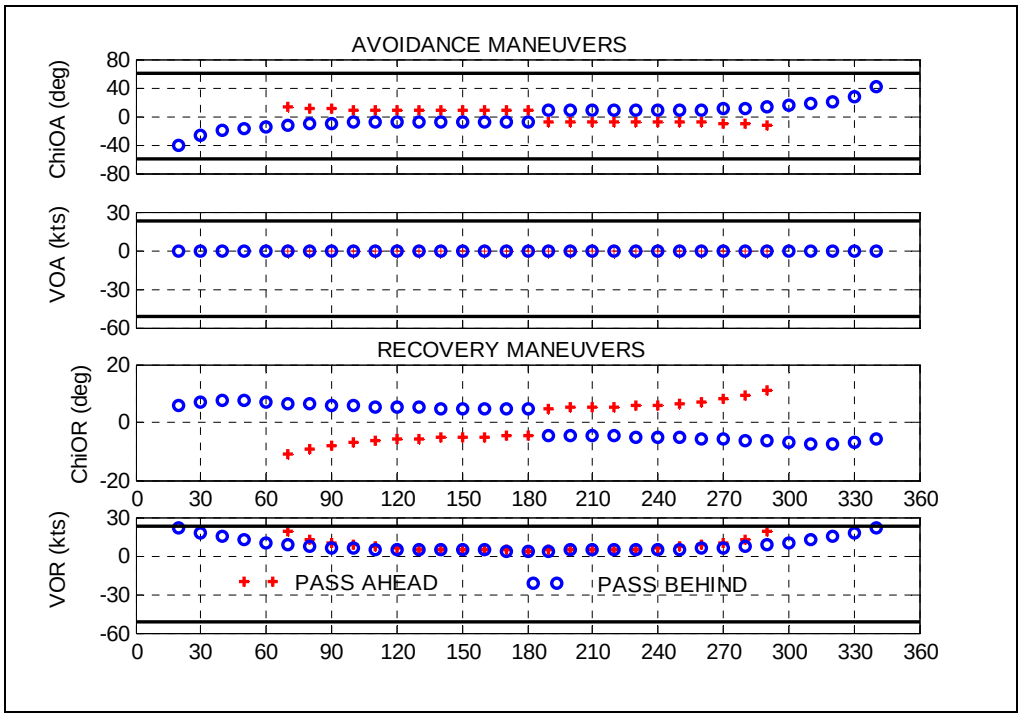

Figure 23. Avoidance and Recovery Maneuver vs Crossing Angle
(Track Angle Avoidance Maneuver, RTA Constraint)

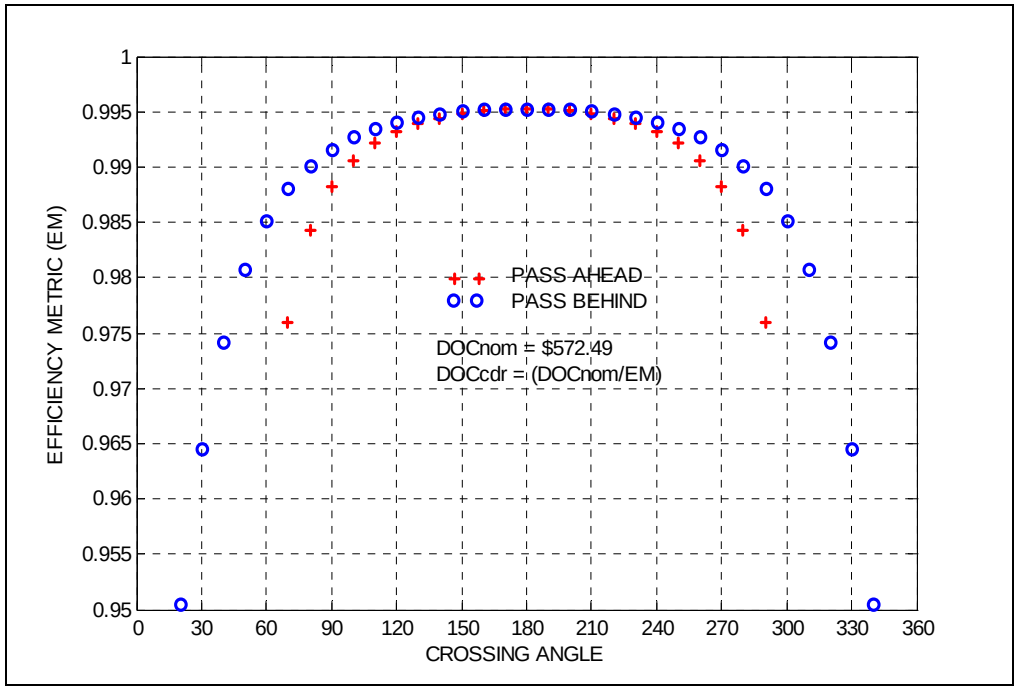

Figure 24. Efficiency Metric vs Crossing Angle
(Track Angle Avoidance Maneuver, RTA Constraint)

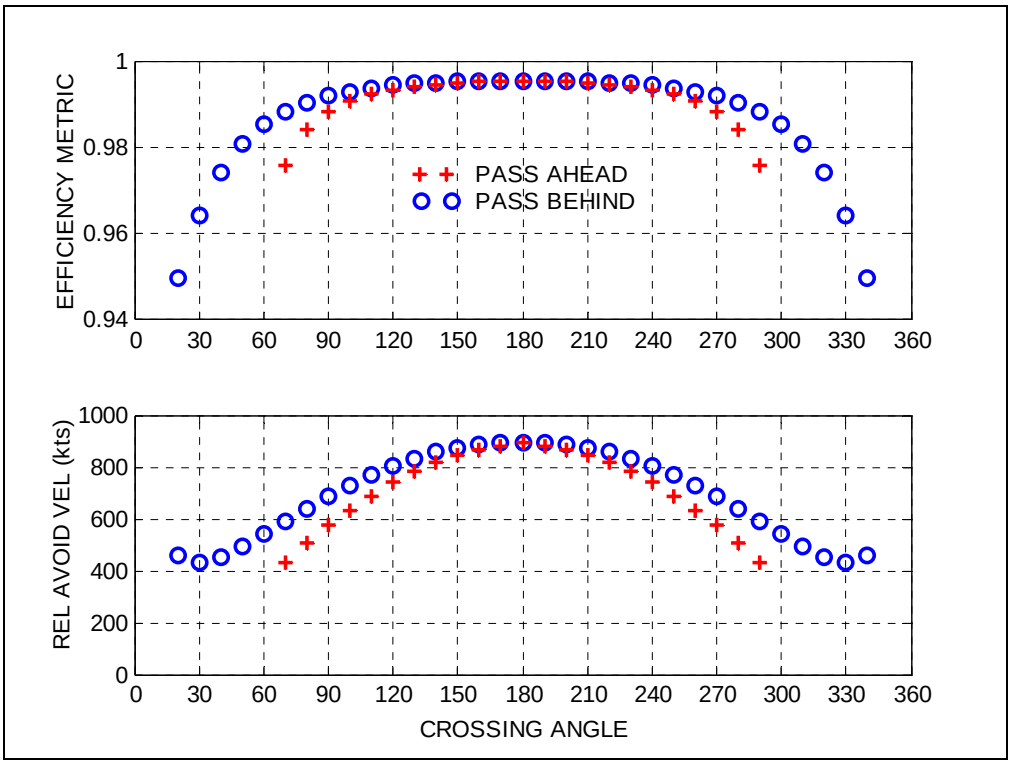

Figure 25. Efficiency Metric and Relative Avoidance Speed vs Crossing Angle
(Track Angle Avoidance Maneuver, RTA Constraint)

Examining Figure 23, it can be seen that the small crossing angle cases (±10 deg) are not feasible. This arises from the fact that the recovery speed limits are exceeded. The reason that these small crossing angle cases are so difficult to perform is that the avoidance relative velocity, $\underline{V}_A$, is smaller, as indicated by the relative avoidance speed in Figure 25. Hence, it takes a recovery speed to achieve the RTA constraint, that is limited by the aircraft speed maneuver envelope.

Based on Figure 24, the pass behind maneuvers provide the highest performance for all feasible avoidance and recovery maneuvers. As shown in Figure 25, the pass behind maneuvers also correspond to the highest relative avoidance speeds.

Figures 26 - 28 present the corresponding optimum avoidance maneuver parametric crossing angle cases. Similar to the track angle avoidance cases, the recovery speed maneuver limits lead to feasible avoidance and recovery maneuvers for crossing angles greater than 20 deg and less than 340 deg.

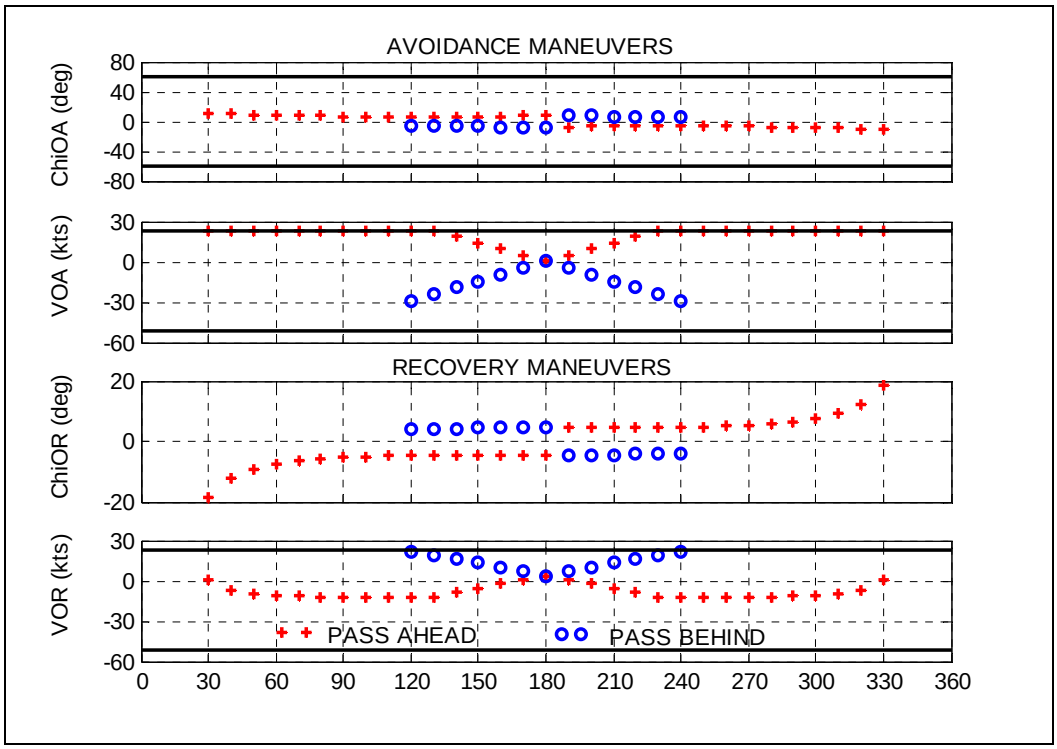

Figure 26. Avoidance and Recovery Maneuver vs Crossing Angle
(Optimum Avoidance Maneuver, RTA Constraint)

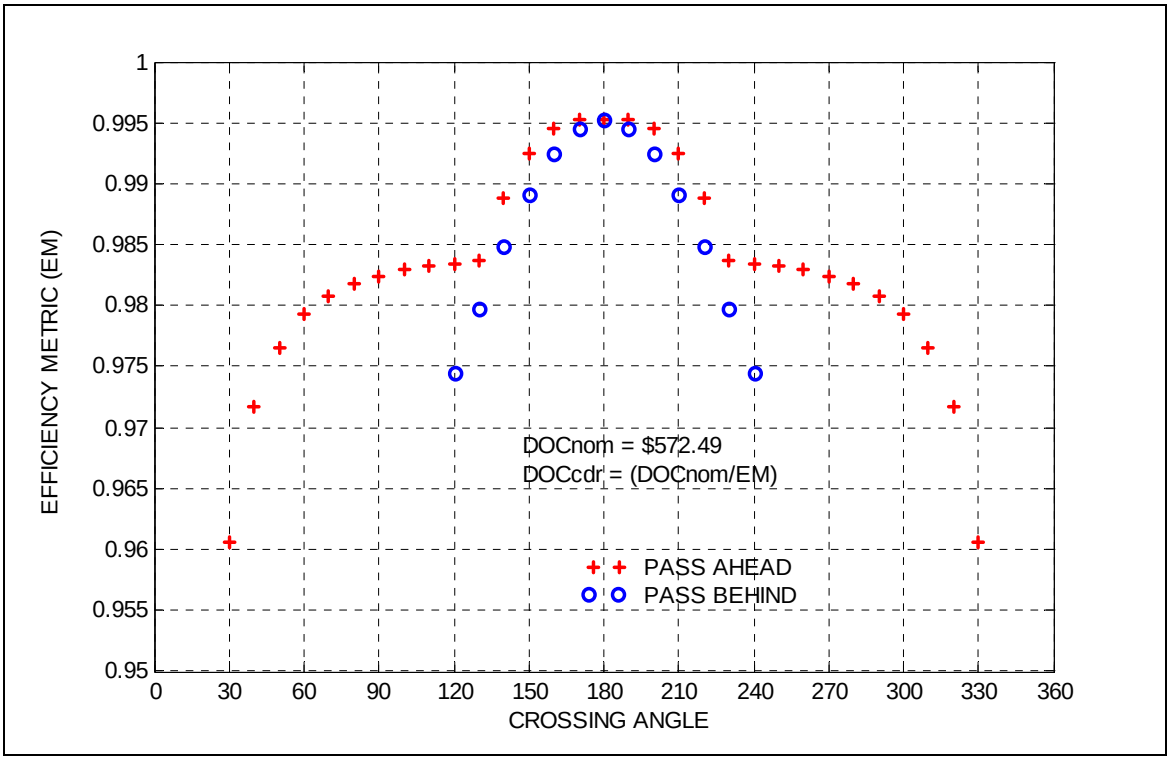

Figure 27. Efficiency Metric vs Crossing Angle
(Optimum Avoidance Maneuver, RTA Constraint)

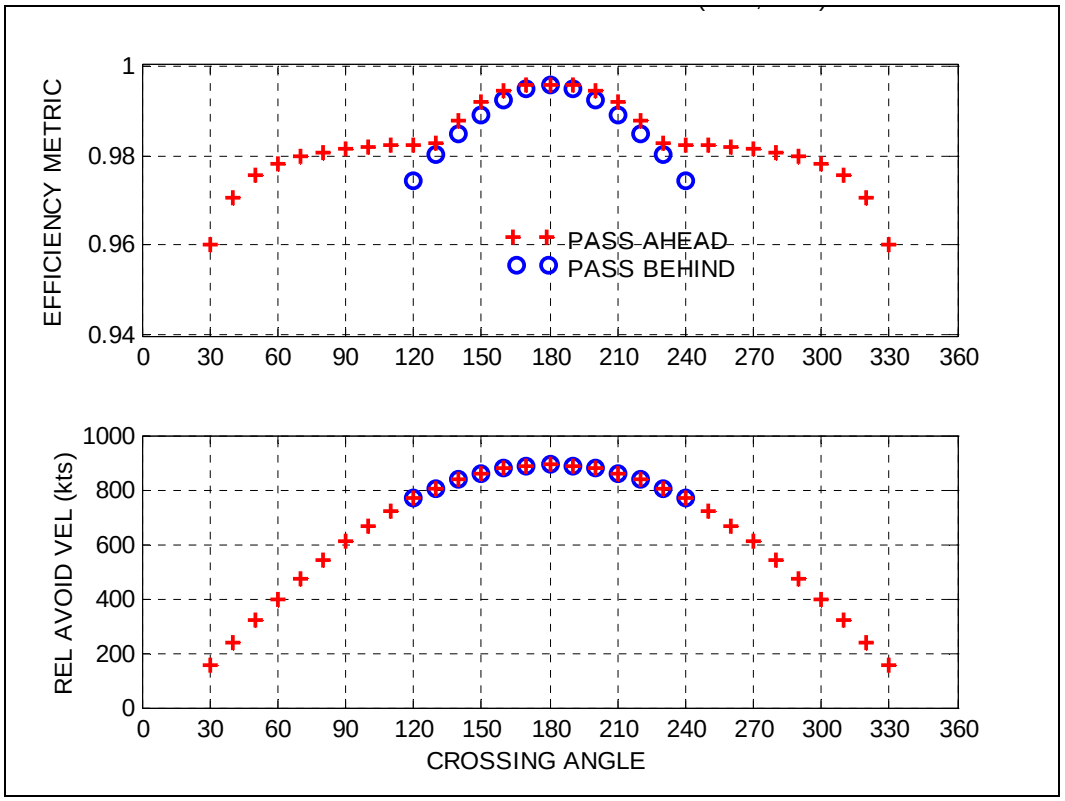

Figure 28. Efficiency Metric and Relative Avoidance Speed vs Crossing Angle
(Optimum Avoidance Maneuver, RTA Constraint)

An examination of Figure 26, shows that the pass ahead maneuvers produce the best perfromance. The unusual bell-shape to the pass ahead performance curve arises from the fact that the avoidance speed maneuvers are constraint by the upper speed limit for crossing angles less than +140 deg or more than +220 deg. Figure 28 shows that the relative avoidance speed is the same for the feasible pass ahead and pass behind maneuvers. Comparing Figure 27 with Figure 24 indicates that the track angle-only avoidance cases outperform the optimum avoidance cases for all but the near head-on crossing angles (170 to 190 deg) where both achieve about the same performance.

10.3 Intruder Avoidance with Recovery to Fixed Waypoint (Speed Ratio: 0.9, RTA Constraint)

In this section the crossing angle cases of the previous section are revisited with the initial condition that the speed ratio, v_O / v_I, is set to 0.9. Hence the intruder aircraft speed is approximately 10% faster than that of the own aircraft. Figures 29 and 30 present the track angle-only avoidance cases while Figures 31 and 32 present the optimum avoidance maneuver cases.

Comparison of these figures with those of the last section indicates the same general trends. Now, however, the feasible track angle only crossing angle cases are limited to track angles greater than 30 deg or less than 330 deg. For the optimum avoidance

maneuver cases, the feasible crossing angle cases are limited to track angles greater than 40 deg or less than 320 deg.

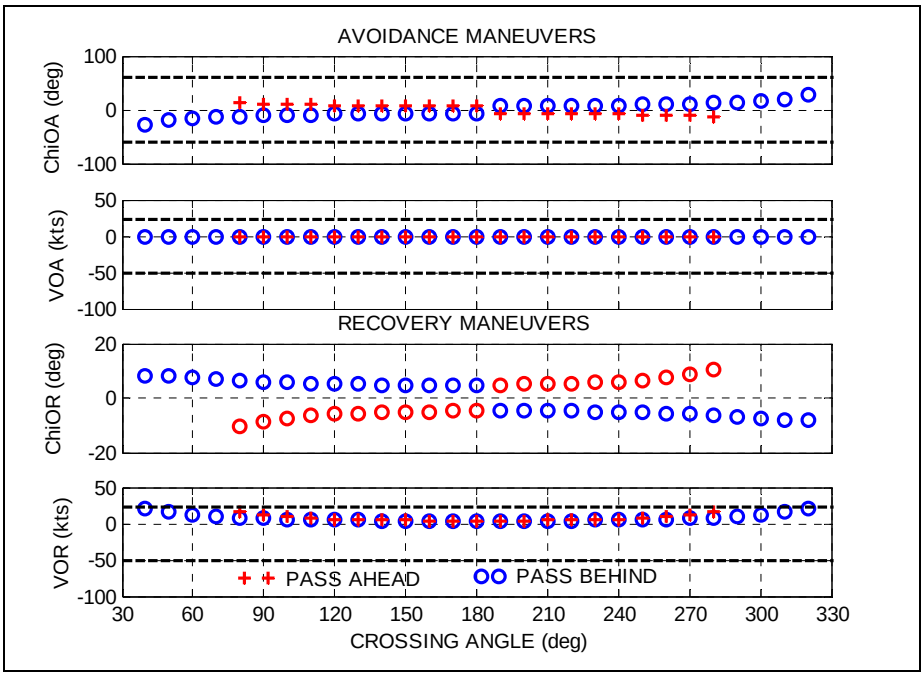

Figure 29. CD&R Maneuvers vs Crossing Angle
(Track Angle Avoidance Maneuver, Speed Ratio vO / vI = 0.90, RTA Constraint)

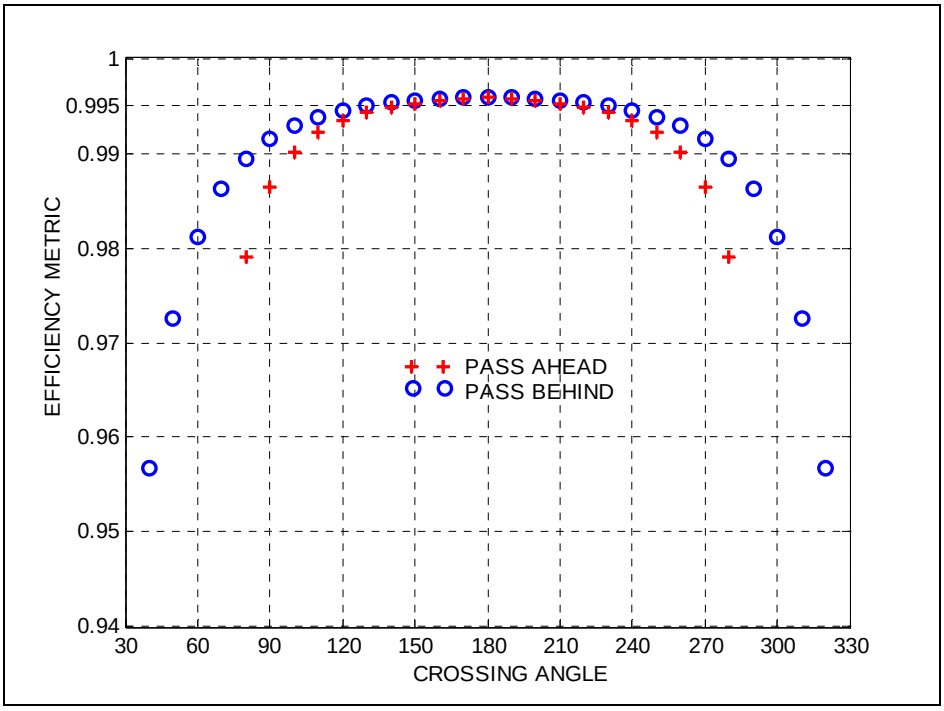

Figure 30. Efficiency Metric vs Crossing Angle
(Track Angle Avoidance Maneuver, Speed Ratio vO / vI = 0.90, RTA Constraint)

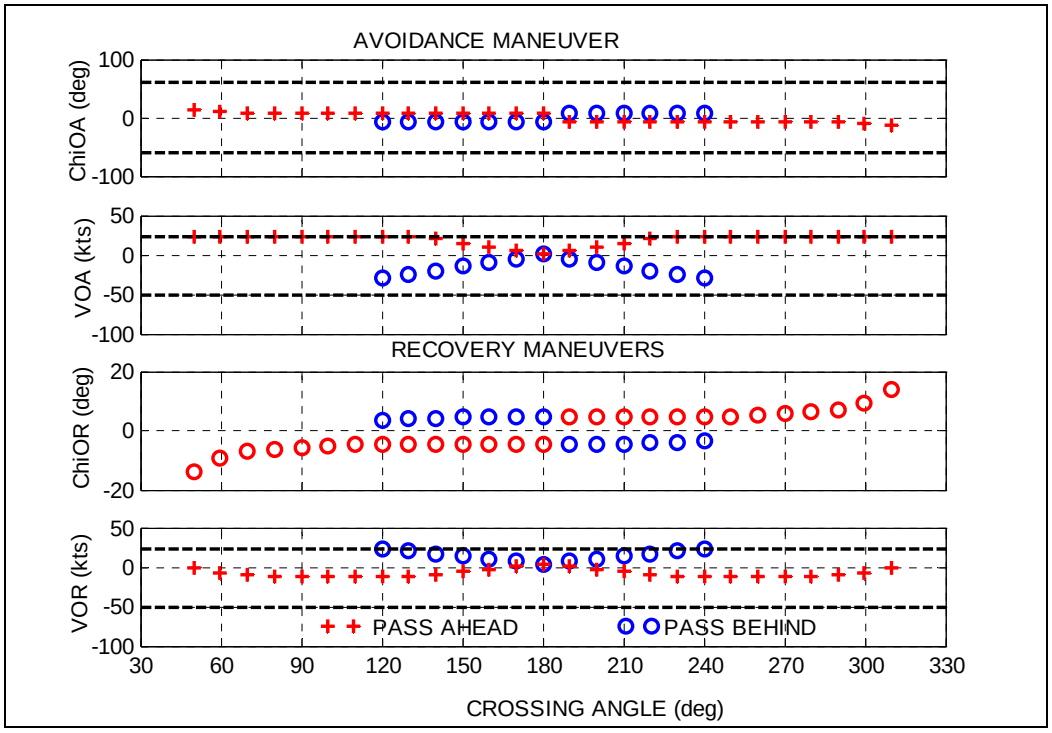

Figure 31. CD&R Maneuver vs Crossing Angle
(Optimum Avoidance Maneuver, Speed Ratio vO / vI = 0.90, RTA Constraint)

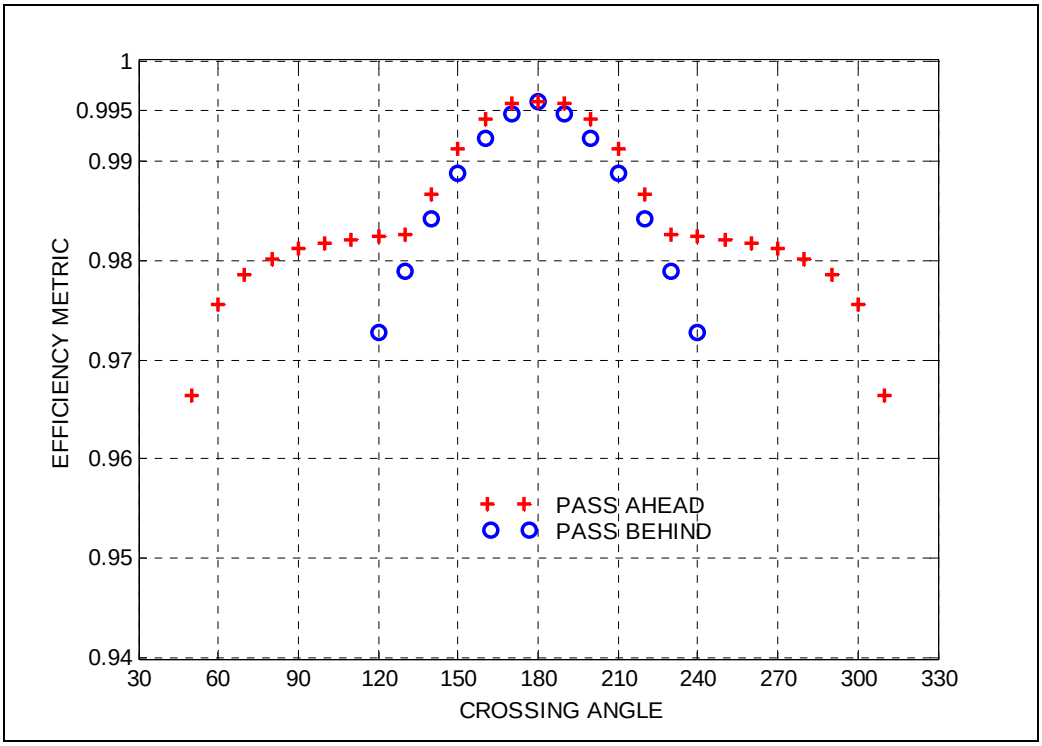

Figure 32. Efficiency Metric vs Crossing Angle
(Optimum Avoidance Maneuver, Speed Ratio vO / vI = 0.90, RTA Constraint)

Comparison of the performance curves in Figures 30 and 32, shows again that the track angle-only avoidance cases outperform the optimum avoidance maneuver cases for all crossing angles except near head on (170 to 190 deg), where they are comparable. Comparison of Figures 30 and 32 with Figures 24 and 27 shows that the, current lower speed ratio cases achieve a generally lower performance than the unity speed ratio cases of the last section except for near head-on crossing angle cases. For the latter the performance is comparable.

10.4 Intruder Avoidance with Recovery to Fixed Waypoint (Speed Ratio: 1.1, RTA Constraint)

Next, the cases for which the speed ratio is 1.1 are investigated. These cases correspond to the initial conditions where the intruder aircraft speed is approximately 10% slower than the own aircraft.

Figures 33 and 34 present the track angle-only avoidance maneuver cases while Figures 35 and 36 present the optimum avoidance maneuver cases. Similarly to the previous two sections, the trend for each set of cases (whether track angle-only or optimum avoidance maneuver) is the same.

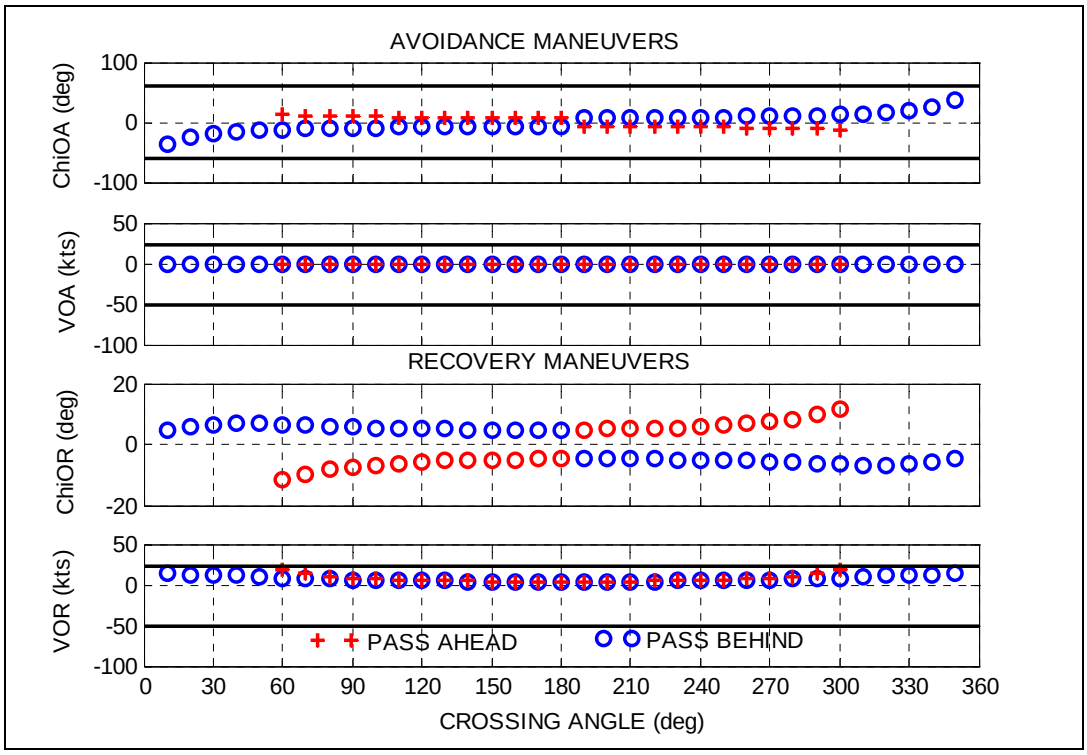

Figure 33. CD&R Maneuvers vs Crossing Angle
(Track Angle Avoidance Maneuver, Speed Ratio vO / vI = 1.1, RTA Constraint)

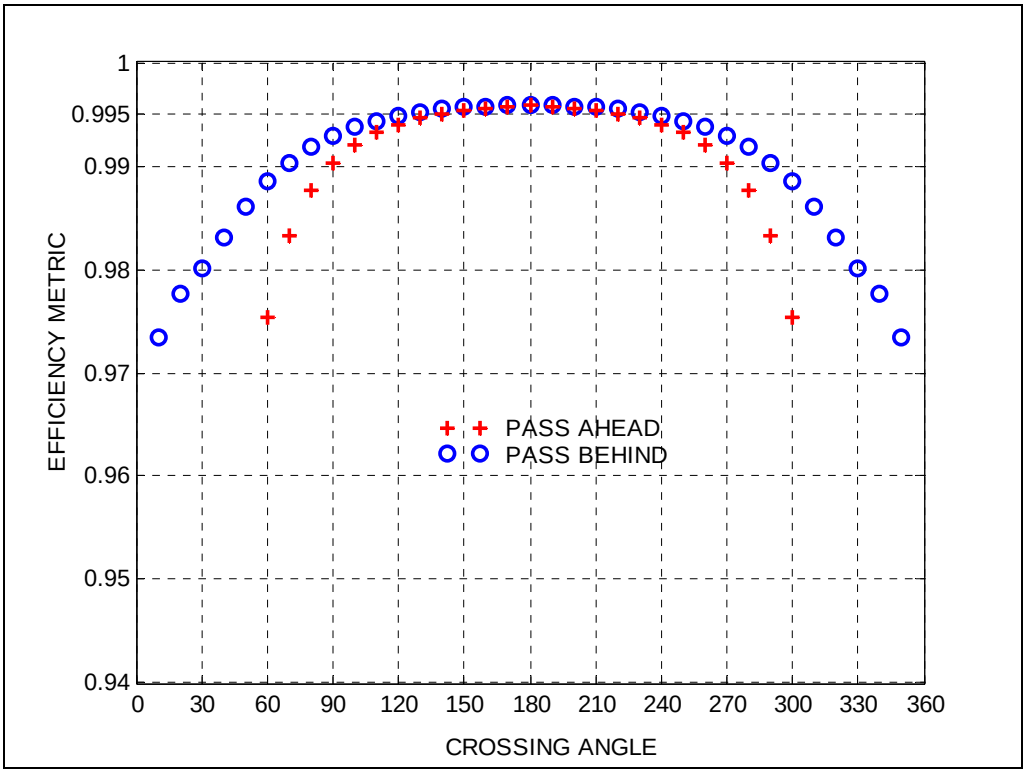

Figure 34. Efficiency Metric vs Crossing Angle
(Track Angle Avoidance Maneuver, Speed Ratio vI / vO = 1.1, RTA Constraint)

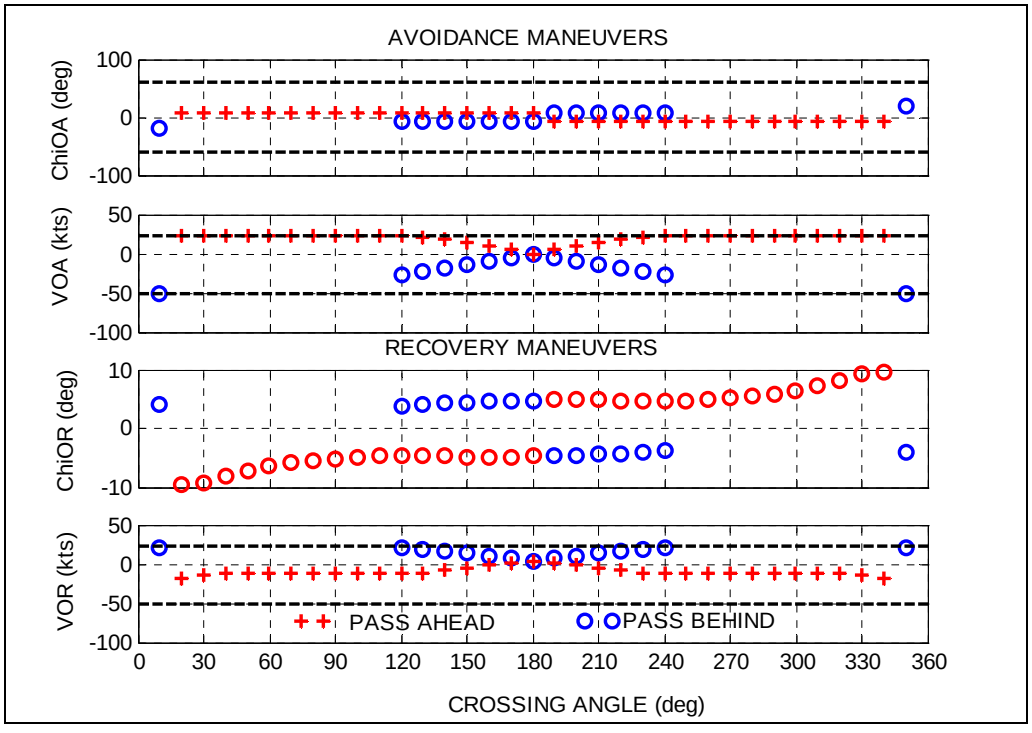

Figure 35. CD&R Maneuvers vs Crossing Angle
(Optimum Avoidance Maneuver, Speed Ratio vO / vI = 1.1, RTA Constraint)

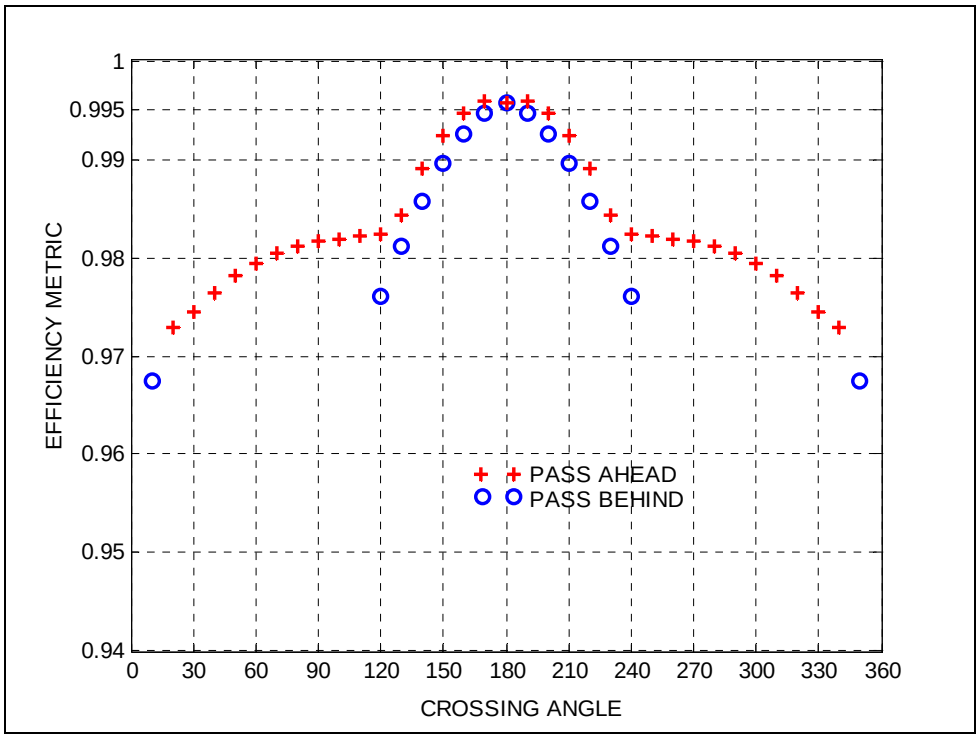

Figure 36. Efficiency Metric vs Crossing Angle
(Optimum Avoidance Maneuver, Speed Ratio vO / vI = 1.1, RTA Constraint)

The feasible maneuvers are limited by the feasible recovery speeds. For the current speed ratio, the feasible maneuvers for both the track angle-only and the optimum avoidance maneuvers include all the crossing angle cases that were investigated (10 to 350 deg). The maximum performance of the maneuvers shown in Figures 34 and 36 are are somewhat higher than for the cases presented in the previous two sections, except for the near head-on cases where they are comparable. It appears that a favorable speed advantage (vO / vI = 1.1) allows the own aircraft primarily to avoid intruder aircraft conflicts with smaller crossing angles (±10 deg) than if the speed advantage is not favorable (vO / vI = 0.9).

10.5 Intruder Avoidance with Recovery to Moving Waypoint (MIT Constraint)

The final parametric cases that are investigated involve the avoidance of an intruder aircraft with recovery to a moving waypoint. Specifically, the own aircraft is in a stream of traffic with a MIT constraint. An intruder aircraft arrives with varying crossing angles (same speed as own aircraft) to produce a potential conflict. The own aircraft performs either a track angle-only avoidance maneuver or an optimum avoidance maneuver before recovering back to its original MIT slot.

Figures 37 and 38 present the track angle avoidance cases while Figures 39 and 40 present the optimum avoidance cases.

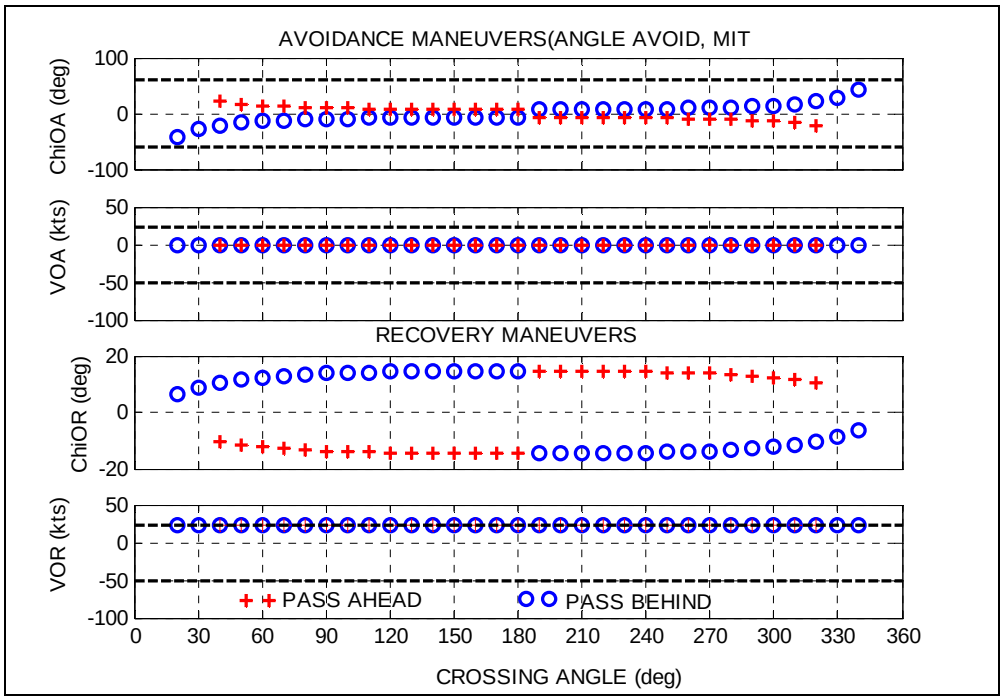

Figure 37. CD&R Maneuvers vs Crossing Angle
(Track Angle Avoidance Manuever, MIT Constraint)

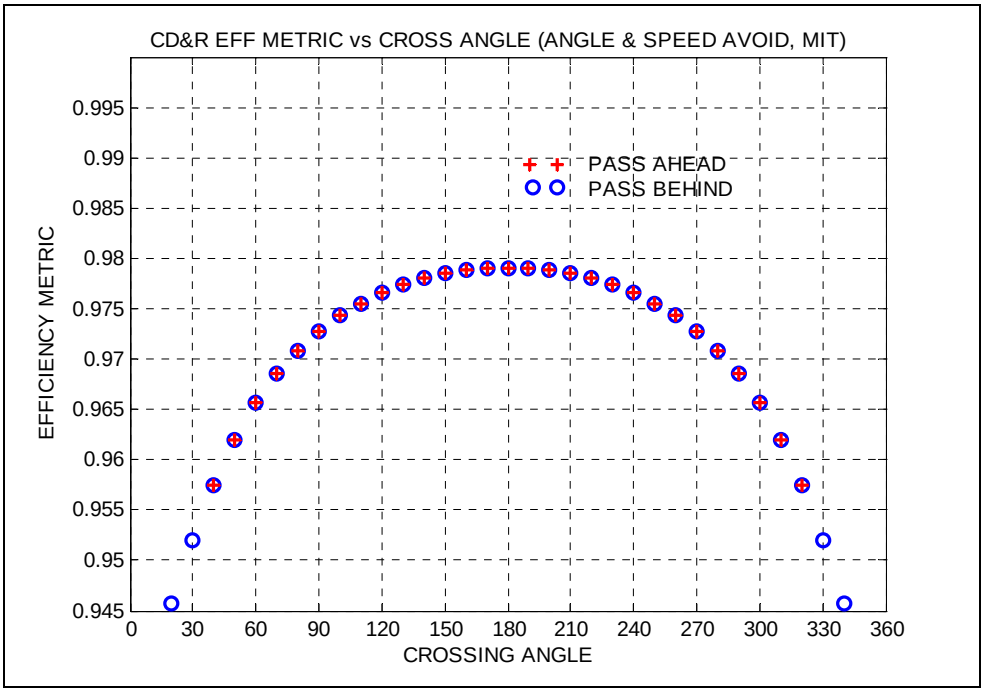

Figure 38. Efficiency Metric vs Crossing Angle
(Track Angle Avoidance Manuever, MIT Constraint)

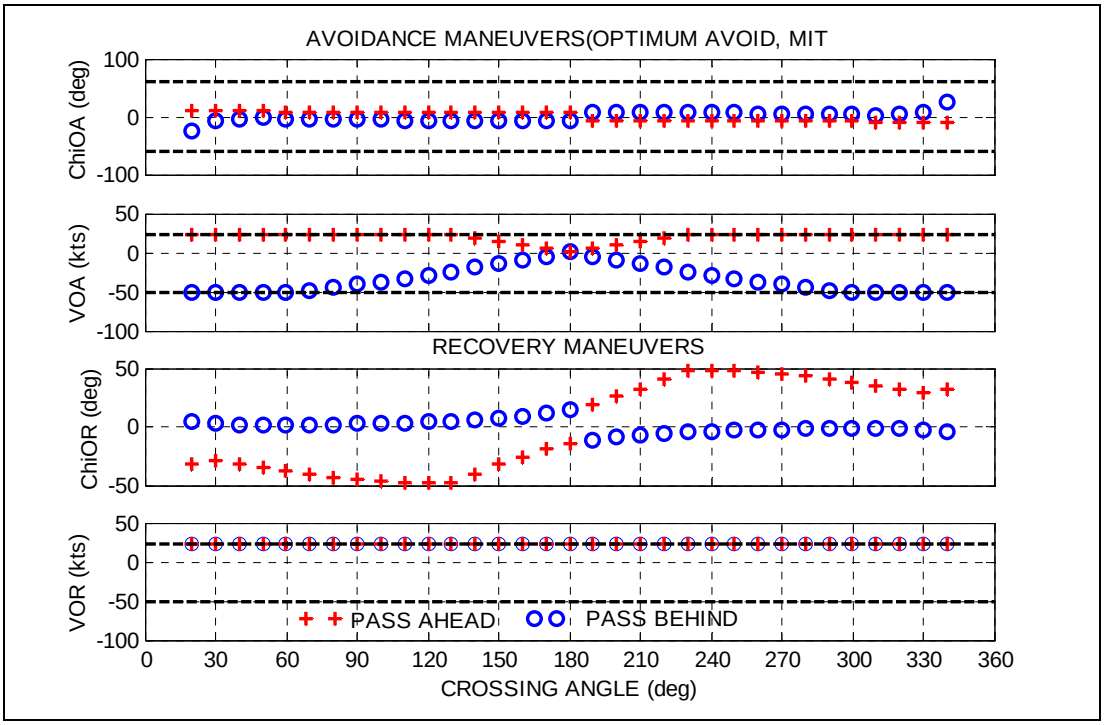

Figure 39. CD&R Maneuvers vs Crossing Angle
(Optimum Avoidance Manuever, MIT Constraint)

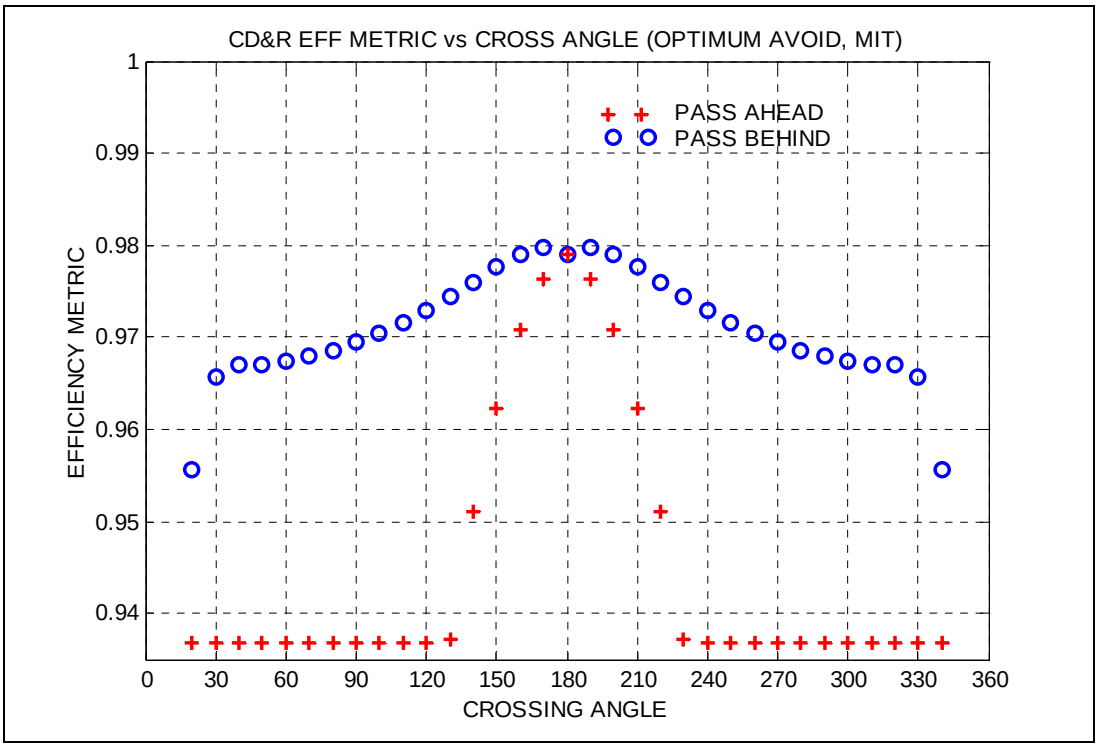

Figure 40. Efficiency Metric vs Crossing Angle
(Optimum Avoidance Manuever, MIT Constraint)

Since the relative recovery speed, V_R, is selected such that the own aircraft returns back to its MIT slot as fast as possible, both sets of maneuver cases are constraint by the maximum feasible recovery speed, v_{OR}. For the optimum avoidance cases, the maneuvers are further limited by the feasible avoidance speeds, v_{OA}.

Examining the efficiency metric for the track angle avoidance case, a very symmetric set of curves are shown that show no difference for the pass behind and the pass ahead maneuvers, where both are feasible. However, the pass behind maneuver cases are feasible down to smaller crossing angles, (20 deg and 340 deg) than the pass ahead cases. As in the previous sections, the track angle avoidance cases outperform the optimum avoidance cases except for nearly head-on encounters (170 to 190 deg) where both are nearly the same.

In Figure 37, the pass ahead cases are limited to crossing angles greater than 30 deg and less than 330 deg, even though these cases do not appear to violate any of the speed or track angle limits. Examination of the relative avoidance speed, V_A, shows that this speed is zero for these infeasible cases.

In Figure 40, the head-on crossing angle case does not result in the highest performance, unlike Figure 38 and the RTA constrained cases. For this MIT scenario the nominal time reach the point at which the conflict resolution is completed is determined as the sum of the avoidance and recovery times, t_A and t_R for this moving waypoint scenario. Hence the nominal time is variable, unlike the RTA cases. An comparison was made of the 180 deg crossing angle case with the 170 deg crossing angle case, in Figure 40. It was established that the relative maneuver DOC was larger for the latter crossing angle case, as expected. However, the nominal DOC was also larger resulting in a slightly better performance for the 170 deg crossing angle case.

The 180 deg crossing angle cases should really be ignored for this scenario since it is unrealistic. Specifically, the intruder aircraft would have to be in the MIT stream of traffic to produce a head-on threat to the own aircraft.

11 Summary and Conclusions

This report presented solutions for conflict avoidance maneuvers that avoid an intruder aircraft or a hazardous region. This was followed by recovery maneuvers that take the aircraft to the next waypoint while conforming to any applicable RTA or MIT constraints. For the avoidance maneuvers, the geometric optimum algorithms of [1] were used. The recovery algorithms incorporated either a miles-in-trail constraint (MIT) or a required time of arrival (RTA) constraint [2] .

A special case was investigated where an aircraft, in a MIT stream of traffic, must perform conflict resolution maneuvers to avoid an intruder aircraft approaching the traffic stream and then return to its MIT slot. In addition, the effect of aircraft performance limits was modeled. The available speed maneuver capability for a typical jet aircraft (e.g., MD-80) at cruise altitude was determined by computing the performance envelope of this aircraft. The impact of these speed limits on solutions for conflict avoidance and/or recovery was studied.

To provide a quantitative assessment and comparison of various conflict resolution maneuvers, a efficiency metric was derived based on the direct operating cost of a maneuver. This efficiency metric reflects both the time and fuel cost of conflict resolution. Performance parameter values to evaluate this cost metric were obtained from the Eurocontrol Base of Aircraft Data (BADA) [6]. These were supplemented with time cost parameters from DOT Form 41 financial data [7] and fuel costs from [8].

The effect of various TFM constraints on the CD&R problem was demonstrated for a 90-deg crossing angle geometry. The TFM constraints considered were: hazard avoidance, capture of a fixed waypoint with and without RTA conformance, and re-capture of a MIT slot. Details of various avoidance and recovery solutions were presented, along with data on the DOC and performance metric.

Speed-only resolutions were found to be generally infeasible. Other resolutions (associated with track angle-only and geometric-optimal avoidance) required speed maneuvers for avoidance and/or recovery. Some of these maneuvers were infeasible due to aircraft performance limits.

Additionally, the impact of finite acceleration, deceleration, and turn rate limitations on feasible maneuvers were studied. In multiple cases, the lack of significant aircraft acceleration capability required an infeasible recovery maneuver that would have resulted in a recovery speed outside of the available speed maneuver margin. In one case, the deceleration limit was a factor, but turn rate limits were never a factor.

In addition to the single crossing angle test cases, parametric crossing angle cases were evaluated for the two aircraft conflict resolution problem. In addition, the initial

intruder speeds were varied such that the own aircraft had a speed advantage / disadvantage of ±10%.

It was found that in general for small crossing angle cases of ±20 degrees or so, the relative velocity between the own and intruder aircraft was so low that any avoidance maneuver that further reduced this relative velocity was generally considered to be infeasible. This was based on the fact that the own aircraft requires such a long time to complete the avoidance maneuver that it passes its next waypoint. As a result it has to make a large recovery maneuver to fly back to this waypoint. Therefore this avoidance and recovery maneuver combination was considered to be impractical.

As for the single crossing angle cases, the track angle-only avoidance maneuvers achieved a higher performance and were generally feasible over a larger range of crossing angle cases than the optimum maneuvers. In the optimum maneuver cases, an avoidance speed change usually led to a more demanding recovery speed (to meet a given RTA) which fell outside the feasible speed maneuver margin. Also, the largest crossing angle cases (180 degrees head-on) achieved the highest performance, with performance deteriorating significantly as the crossing angle decreases. The closer to head-on (180 deg) the conflicts were, the smaller were the differences in resolution performance between both the track angle-only and optimum maneuvers and between the pass ahead and pass behind maneuvers.

Of the parametric cases that involved different initial speeds, the highest performance was achieved for the case where the own aircraft initial speed advantage was 10% higher than the intruder aircraft. In addition, feasible avoidance maneuvers could be found for all the crossing angle cases that were evaluated for this scenario.

The reverse was true when the own aircraft had a speed disadvantage of 10%. For this case, the feasible range of crossing angle cases were the most limited, being restricted to crossing angles > 30deg and < 330 deg. In addition, the non-head on crossing angle cases had the lowest performance.

For the crossing angle parametric cases, it was shown that the track angle-only avoidance maneuvers that required the aircraft to pass behind an intruder aircraft tended to outperform the cases where the own aircraft passes ahead of the intruder aircraft. For the optimum avoidance maneuver cases, the reverse was true.

Further work is recommended to extend the analysis of this report to include the altitude plane. As a result, horizontal conflicts could be avoided using speed, track angle, altitude, or any combination of these avoidance maneuvers. In addition, this altitude extension would investigate the more challenging conflict problems where the own aircraft finds itself in conflict with an intruder pop-up aircraft or the own aircraft encounters a conflict with an intruder, while it is changing altitude. The efficiency metric would then be extended to select the optimum avoidance maneuver.

This work should also be extended to include uncertainties in the knowledge of the position and velocity of the intruder aircraft. Hence, for longer range (strategic) detection of conflicts, the own aircraft has a choice of delaying the initiation of the avoidance maneuver until the intruder state uncertainty has been reduced. Alternately, the avoidance maneuver can be initiated directly after detection. In the former case, the required avoidance and recovery maneuver may be larger than if the avoidance maneuver had been initiated earlier. In the latter case, the avoidance maneuver may not be as efficient or possibly even necessary.

12 References

[1] Bilimoria, K.D., "A Geometric Optimization Approach to Aircraft Conflict Resolution," Paper No. 2000-4265, AIAA Guidance, Navigation and Control Conference, August 2000.

[2] Bilimoria, K.D. and Lee, H.Q., "Aircraft Conflict Resolution with an Arrival Time Constraint," Paper No. 2002-4444, AIAA Guidance, Navigation and Control Conference, August 2002.

[3] Anon., " United Airlines B-747-400 Captain and First Officer Manual," Jeppesen Sanderson, 20 September 1996.

[4] Bilimoria, K.D., " Compensating for Maneuver Dynamics," NASA Ames Research Center, 13 May 2002.

[5] DC-9 Performance Branch, *Model DC-9 Series 80 Performance Handbook, JT8D-209 Engine*, Report Number MDC J8757, Revision Date February 1984, Revision Letter C, McDonnell Douglas Corporation.

[6] Anon, "User Manual for the Base of Aircraft (BADA), Rev. 3.1," Eurocontrol, EEC Note No. 25/98, November 1998.

[7] Anon, "Aviation System Analysis Capability (ASAC) Database," Logistics Management Institute, http://www.asac.lmi.org, January 2002

[8] Anon, "Fuel Cost and Consumption," Bureau of Transportation Statistics, http://www.bts.gov/oai/fuel, May 2001.

[9] Anon, "US Standard Atmosphere 1976," National Oceanic and Atmospheric Administration, 1976.

[10] Multiple pilot replies to “En Route Cruise Slowdown” email, www.bluecoat.org, June-July 2002.

Appendix A: MD-80 Cruise Performance Characteristics

This appendix summarizes the performance of the MD-80 aircraft based on [5]. The focus is on the MD-80 aircraft operating at a cruise pressure altitude of 31,000 ft with a weight of 135,000 lb. The data contained in this appendix is provided primarily in support of computing the efficiency metric to evaluate candidate avoidance and recovery maneuvers. In addition, some of the material presented illustrates the penalties / benefits when a maneuver results in a change from the nominal cruise speed and track angle.

The aerodynamic drag coefficient values at different cruise speeds and for different coordinated turn maneuvers were obtained from curves provided by [5]. To derive an analytic function for the drag coefficient, a fourth order polynomial fit was made through the data points for three different cruise conditions. These cruise conditions consist of level flight, a nominal coordinated turn, and a maximum coordinated turn. The polynomial equation is of the form:

$$C_D(v) \cong (0.01)\left[a_4\left(\frac{v}{100}\right)^4 + a_3\left(\frac{v}{100}\right)^3 + a_2\left(\frac{v}{100}\right)^2 + a_1\left(\frac{v}{100}\right) + a_0 \right] \qquad \text{(A-1)}$$

In (A-1), the drag coefficient is C_D, the true airspeed is v, expressed in units of ft / sec, and the polynomial coefficients are a_i. The polynomial coefficients are summarized in Table A-1 and the corresponding drag coefficient curves are illustrated in Figure A-1

Table A-1. MD80 Drag Coefficient Polynomial Fit Parameters

Cruise Flight Segment	Polynomial Coefficients				
	a_4	a_3	a_2	a_1	a_0
Level Flight	0.351134	-9.67877	100.318	-464.171	813.608
Coordinated Turn (1 deg / sec Rate)	0.600597	-16.6981	174.336	-810.910	1422.76
Coordinated Turn (35 deg Bank Angle)	0.566609	-15.4076	157.353	-716.738	1235.13

The 1 deg / sec turn is a typical turn used in cruise that results in a change in track angle with minimum disturbance to the passengers. The 35 deg bank angle turn, however, is used to perform an avoidance maneuver under tactical conditions where there are only a few minutes of time to avoid a conflict. For the cases presented in the main body of this report, the 35 deg bank angle turns were used.

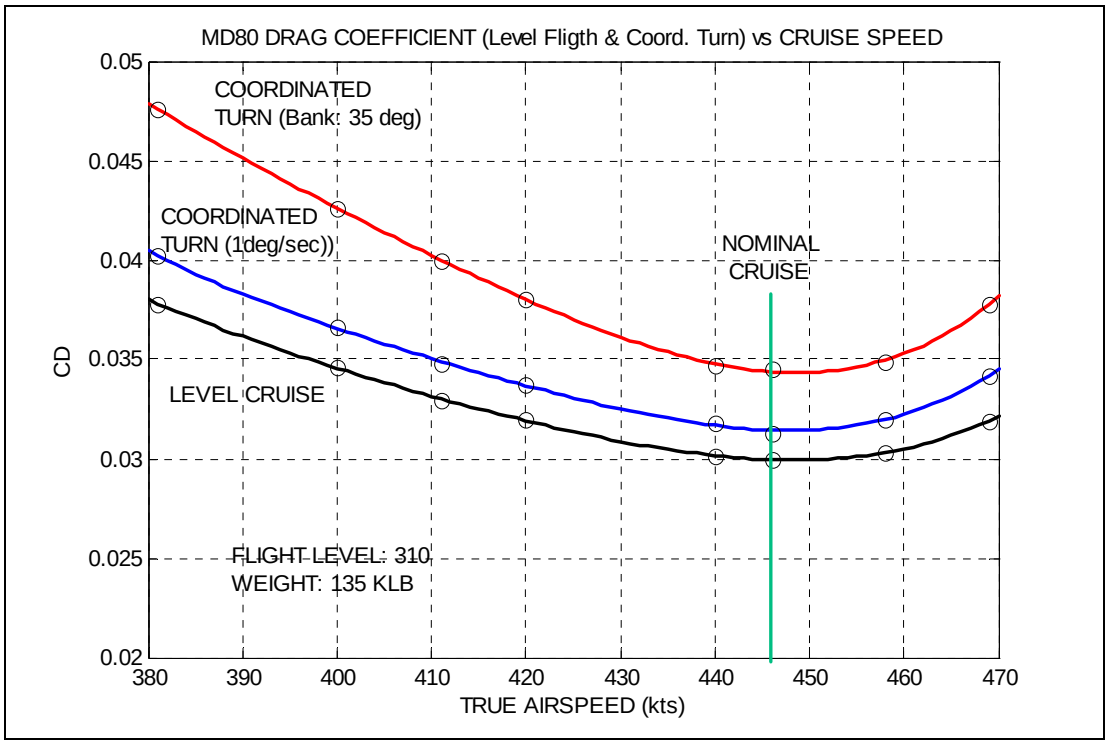

Figure A-1. MD-80 Cruise Drag Coefficient vs True Airspeed
(FL 310, Weight 135Klb)

Using the drag coefficient curves in Figure A-1, the drag curves are illustrated in Figure A-2 for different maneuvers as a function of the true airspeed.

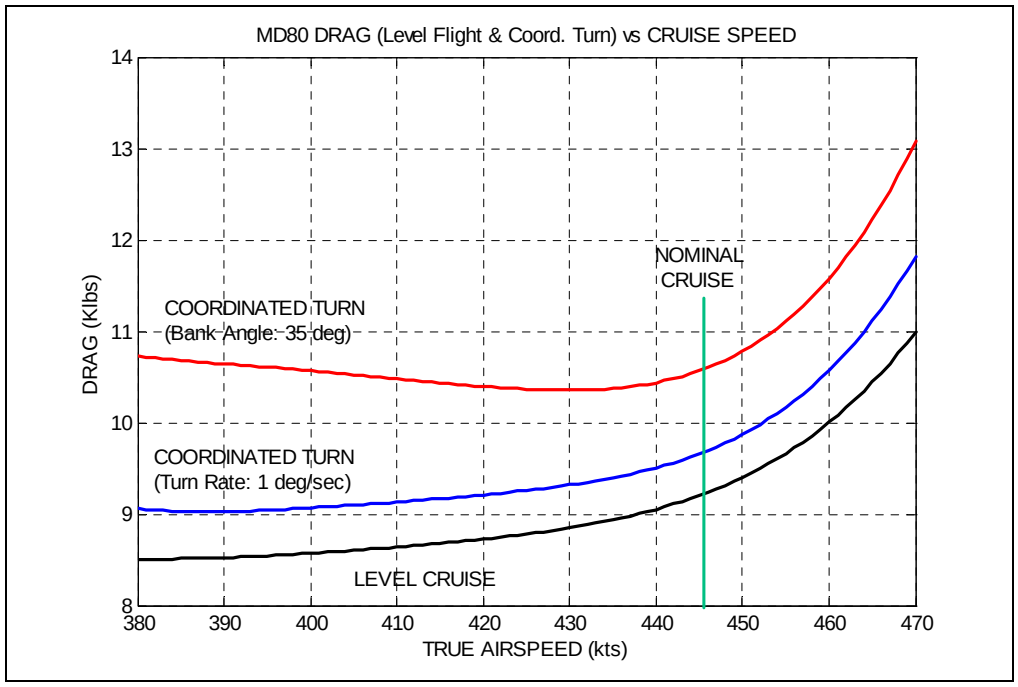

Figure A-2. MD-80 Cruise Drag vs True Airspeed
(FL 310, Weight 135 Klb)

While the nominal cruise speed of Mach 0.76 or 446 kts produces the minimum drag coefficient in Figure A-1, the minimum drag airspeed is at slower speeds than the nominal cruise speed as shown in Figure A-2.

The direct operating cost per distance traveled for level flight is illustrated in Figure A-3 while Figure A-4 focuses only on the fuel cost per distance. As shown in Figure A-3, the nominal cruise speed is slightly lower than the minimum while in Figure A-4, the nominal cruise speed is considerably higher than the minimum.

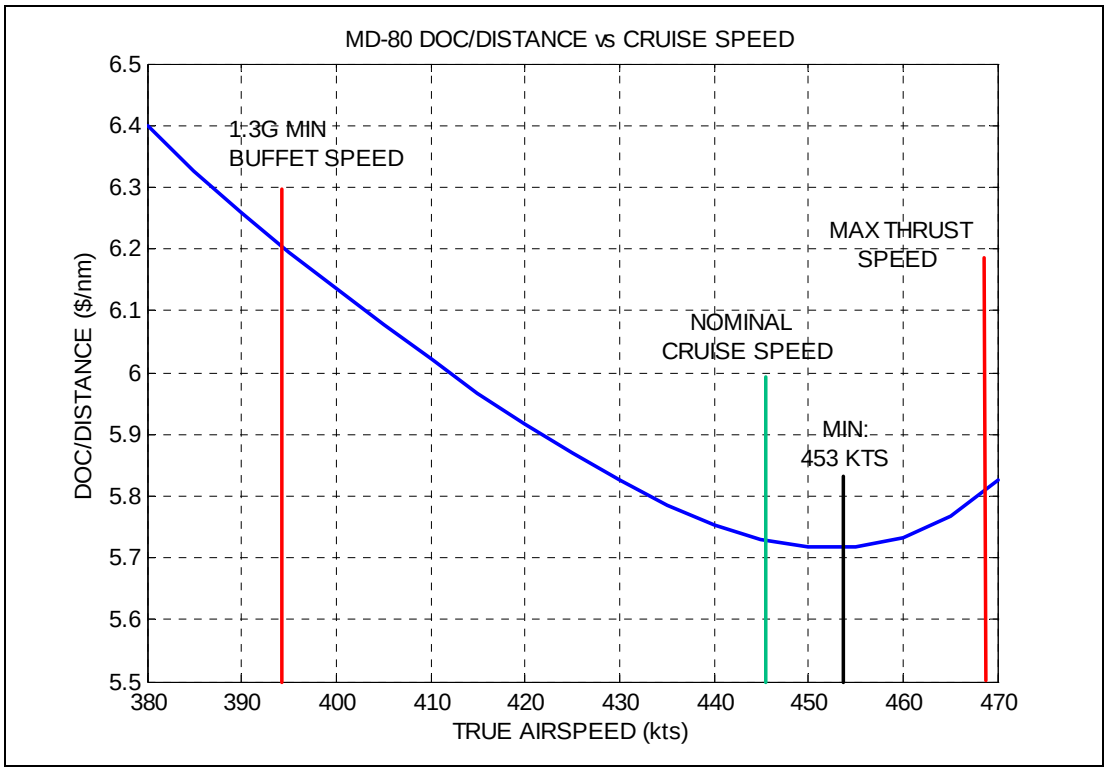

Figure A-3. MD-80 Total Direct Operating Cost/Distance vs True Airspeed
(FL 310, Weight: 135 Klb)

In selecting the operating cruise speed for the MD-80, [5] uses the reciprocal curve to Figure A-4, as shown in Figure A-5. Figure A-5 presents the distance traveled per weight of expended fuel.

The select the preferred cruise speed, the maximum distance/fuel weight is selected in Figure A-5. Next the 99% value of the maximum distance/fuel weight that lies to the right of the true airspeed corresponding to the maximum distance/fuel weight is found. Then the cruise speed is selected as the minimum of either the 99% value of 438 kts or Mach 0.76 (446) kts. In this study, 446 kts was used instead of 438 kts, partly to be consistent with the BADA database.

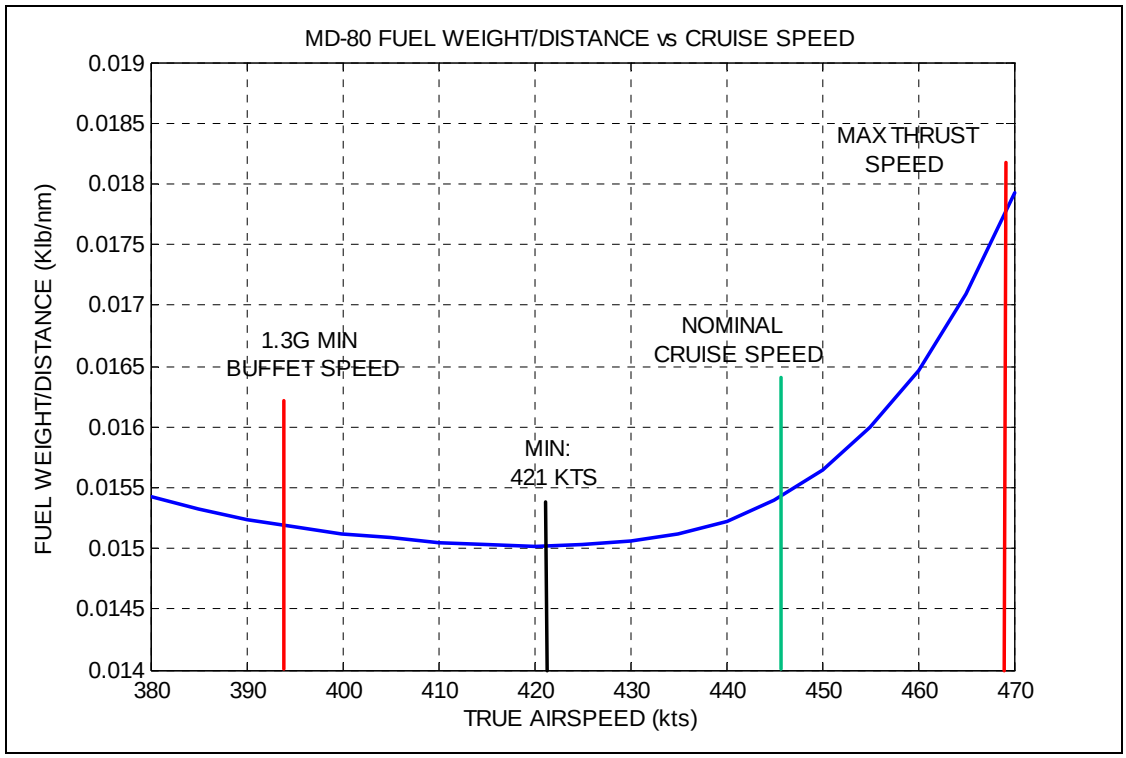

Figure A-4. MD-80 Fuel Weight/Distance vs True Airspeed
(FL 310, Weight: 135 Klb)

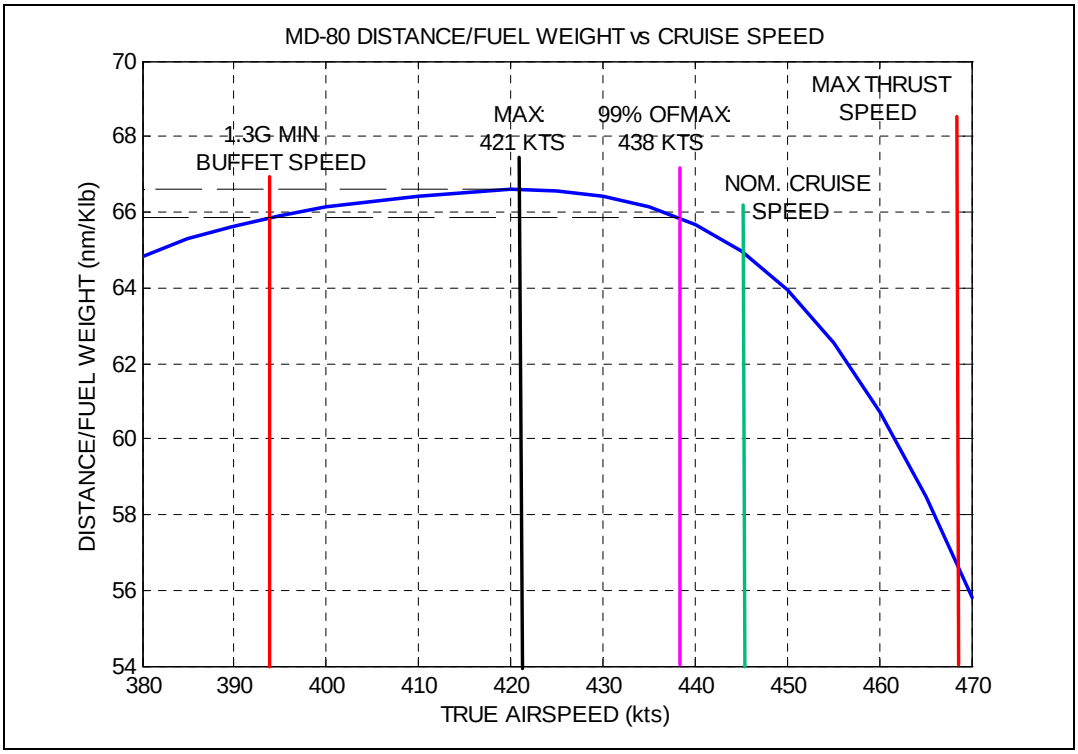

Figure A-5. MD-80 Distance /Fuel Weight vs True Airspeed
(FL 310, Weight: 135 Klb)